Vessel motion based criteria for pipeline Abandonment and Recovery operations

R. K. Sri Paravastu

Technische Universiteit Delft

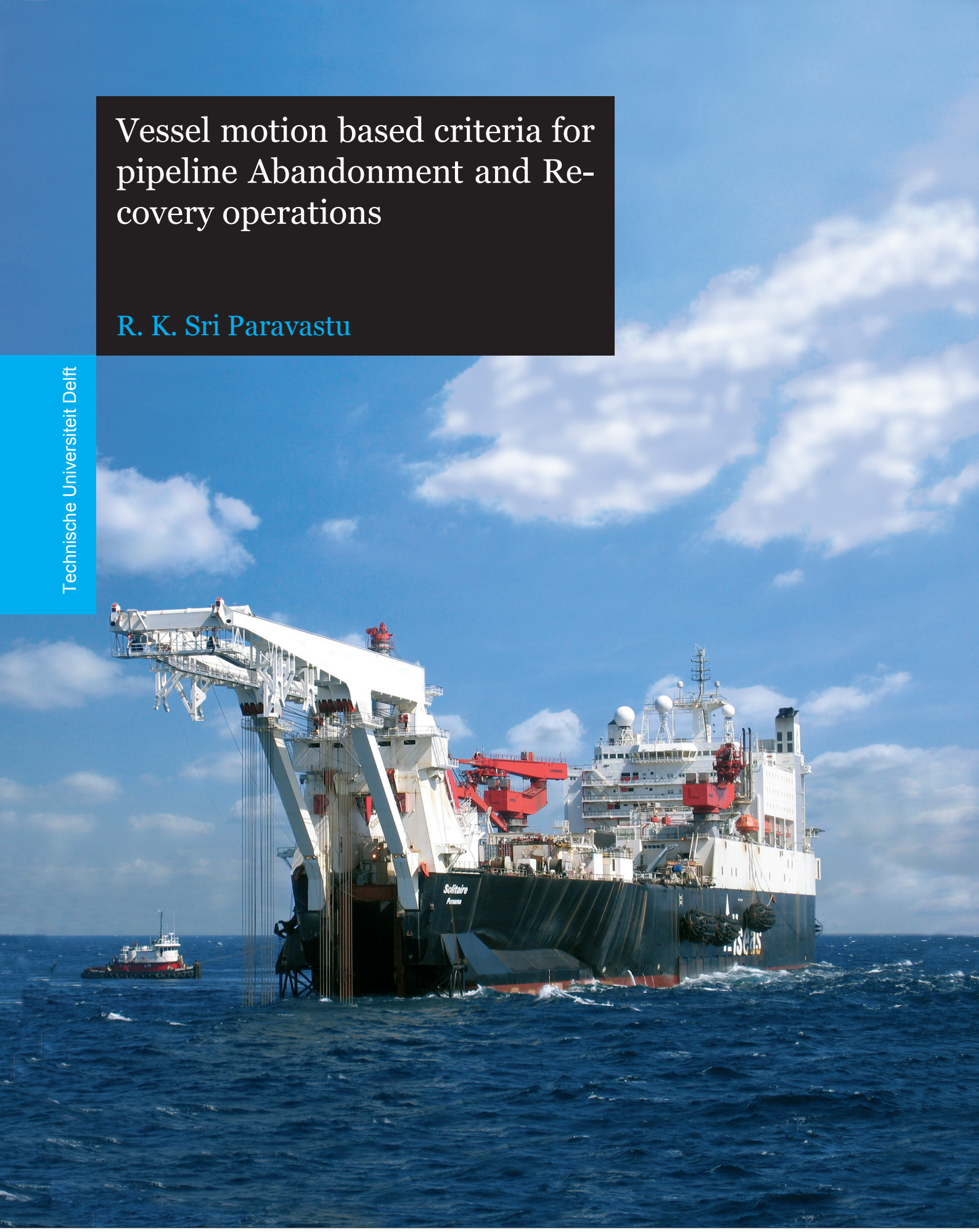

TU Delft Delft University of Technology

Allseas

Challenge the future

Vessel motion based criteria for pipeline Abandonment and Recovery operations

by

R. K. Sri Paravastu

to obtain the degree of Master of Science
at the Delft University of Technology,
to be defended publicly on Tuesday October 4, 2016 at 14:00 Hrs.

Student number:	4387171	
Personal email:	r.k.sriparavastu@hotmail.com	
Project duration:	December 7, 2015 – October 04, 2016	
Thesis committee:	Prof. dr. ir. R. H. M. Huijsmans,	TU Delft, Committee Chairman
	Dr. ir. Peter Wellens,	TU Delft, Supervisor
	Dr. eng. François Gerspach,	Allseas Engineering, Supervisor
	Prof. dr. ir. Pieter van Gelder,	TU Delft, Committee member

This thesis is confidential.

An electronic version of this thesis is available at http://repository.tudelft.nl/.

TU Delft Delft University of Technology

Allseas

Abstract

Offshore pipeline installation is limited by pipeline integrity during the laying process. Pipeline integrity is evaluated with the help of buckling checks, which help determining the feasibility of pipeline installation for a given sea condition. The operational limit of pipeline installation is determined during project preparation, by outlining a limiting sea condition (A standard, uni-directional wave spectra) beyond which pipeline damage is assumed to occur. Therefore, the installation process is interrupted during such a sea condition and the pipe is abandoned. The pipe is recovered when the weather improves, for further installation. This entire process is termed as *Abandonment and Recovery* (A&R) operation.

In reality, the offshore sea conditions encountered during operation are different in nature, when compared to the sea-state outlined during project preparation (non-standard, multi-directional sea spectrum). This creates an uncertainty in the decision making process for pipeline *abandonment*. In order to overcome this, an A&R criterion is desired, which is insensitive to the sea-state definition. The criterion should be based on vessel motion parameters.

The goal of this thesis is to predict the extreme response of pipeline based on vessel motions, in order to evaluate the integrity of pipeline for a given environment. Three statistical models were developed during the course of the study, to predict the extreme responses of pipeline using one or more input parameters among all the vessel motions; for a given installation case. These models require the generation of a database for each installation case, the output of which results in predictive formulas with a certain degree of confidence.

The report consists of two main parts. The first part describes in detail, the procedure employed for a given installation case, right from database generation to data gathering and post-processing analysis, resulting in three statistical models that predicts the extreme response in the sagbend part of the suspended pipeline. This procedure/method has been generalised for any type of installation case (small and large water depths, flexible and stiff pipelines).

The second part of the report shows the results of the procedure, for two sample installation cases; one in deep water and the other in shallow water. The models are validated for different kinds of randomly chosen sea-spectra, that are assumed to be representative of the offshore environment. This is then followed by the analysis of results and discussions about various aspects of the procedure, adopted in this research.

Keywords: Offshore pipelines; vessel motions; S-lay method; pipeline integrity; sagbend; statistical modelling; multiple regression; deep water pipelay; shallow water pipelay; Orcaflex; OFFPIPE;

Acknowledgements

This report is an elaboration of the work done during my graduation thesis, in partial requirement for my Master of Science degree in Offshore and Dredging Engineering, at Delft University of Technology. The duration of the thesis lasted 10 months (07/12/2015 - 04/10/2016) at the Pipeline engineering department in Allseas Engineering B.V., Delft. Allseas Engineering is the sponsor of my thesis study and its support is gratefully acknowledged.

First of all, I would like to thank my supervisor, Dr. eng. François Gerspach, who guided me through every step of the way, and was always available to answer my questions. He instilled the knowledge and the thought process in me, which is what led to the successful completion of this thesis study. I wholeheartedly thank him for his cooperation and support. I would like to thank Patrick Rijneveld from Allseas, who trusted in me and gave me the opportunity to work for Allseas engineering. He also provided me with valuable insight into the practical aspects related to my study. I would like to thank Sytske de Groot from the naval department in Allseas, who provided me the data required for my study and was also available to answer any questions I had, regarding the metocean aspects of my study. I would also like thank all my colleagues from the Pipeline Engineering department, as well as my friends from the other departments within Allseas, who created a friendly working atmosphere during my time at the company.

Apart from the people in Allseas engineering, I would like to thank the people from TU Delft who had a contribution to the final result of my thesis study. I would firstly like to thank my committee chairman, Professor Rene Huijsmans for his cooperation and support. I would like to thank my supervisor Dr. ir. Peter Wellens for providing me with the right feedback and support, and for overseeing the progress of my thesis study. I would like to thank all my colleagues and friends from the university, for all the memorable moments during my journey in becoming a master student. I would finally like to thank Professor Pieter van Gelder, for being a part of my thesis committee.

This work is dedicated to my parents and my girlfriend, for their unconditional love and support. They are the backbone for all my achievements in life.

R. K. Sri Paravastu
Delft, September 2016

Contents

1 Introduction

The first part of this chapter will give a brief introduction about Allseas engineering and its various activities, with a major focus on the S-lay method of pipeline installation. The subsequent section introduces the problem under study and defines scope of the thesis.

1.1. Allseas engineering B.V.

This thesis is sponsored by Allseas Engineering B.V. which belongs to Allseas Group S.A.; one of the leading companies for offshore pipeline installation and subsea construction services. The company was founded in 1985 by Edward Heerema, and has massively progressed since then. Allseas group is also expanding its expertise to the areas of platform installation and decommissioning.

There are currently five pipelay vessels owned and operated by Allseas namely, Lorelay, Solitaire, Audacia, Tog mor and the Pioneering Spirit. All the vessels use the *S-lay* method of pipeline installation. With about 30 years of experience and having one of the most versatile fleet of vessels, Allseas can lay a wide range of pipes in an even wider range of water depths. Solitaire is the vessel used for all the analyses presented in this thesis study.

1.2. S-lay method

There are many methods of installing offshore pipelines. The most common methods are S-lay, J-lay and reel-lay. Reel lay is mainly used for flexible pipelines and small diameter steel pipelines. The pipelines are reeled onto a large roller and installed offshore by un-reeling the pipeline under tension. J-lay and S-lay are similar methods which are used for large diameter steel pipelines. Unlike reel-lay, both S-lay and J-lay methods require the pipeline to be constructed offshore. The difference between the S-lay and J-lay methods are well documented in literature[11]. This section will describe in detail, the S-lay method of pipeline installation.

In the S-lay method, the pipe is constructed in various workstations, positioned horizontally along the length of the vessel (figure 1.1). These line of stations is called the *firing line*. The pipe joints entering the firing line are first welded onto the existing pipeline. Once welded, the pipe is moved over roller supports to the subsequent workstations, where the joint is coated and the weld quality is tested. The pipe is transferred to the next workstation by moving the vessel forward. At the end of the firing line, the pipe enters a truss shaped structure which extends from the vessel, known as the *stinger*. It usually consists of separate sections hinged

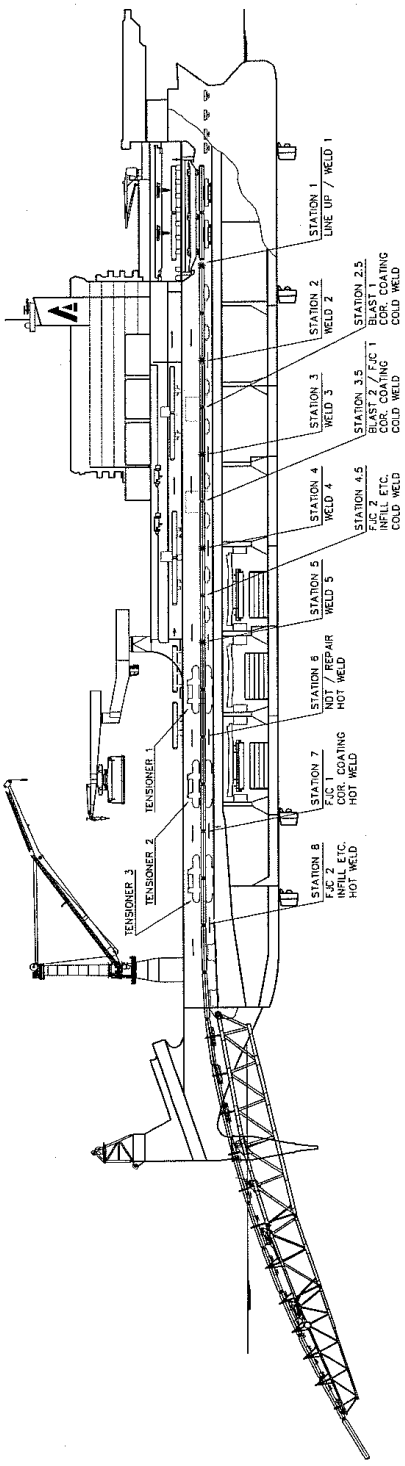

Figure 1.1: Solitaire’s firing line

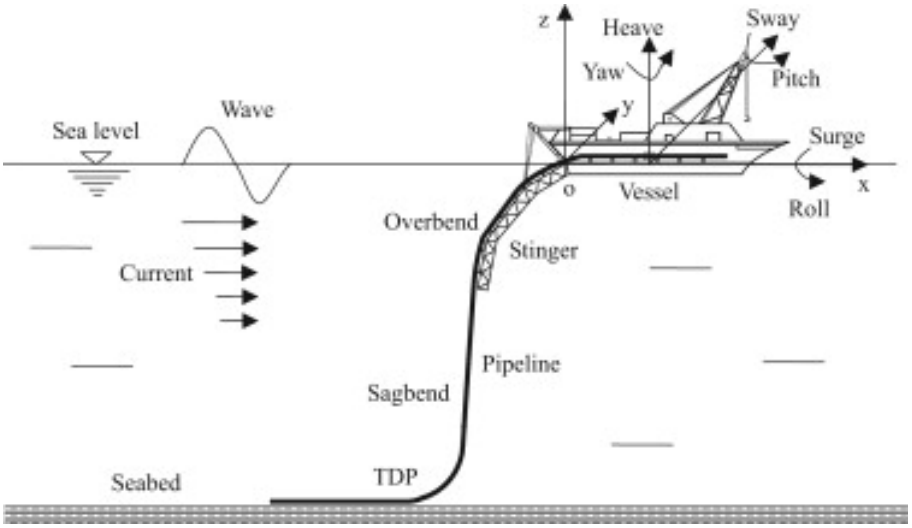

Figure 1.2: Deep water pipelay

to each other, such that they can be rotated into an arc of desired radius. The main purpose of a stinger is to direct pipe towards the sea floor, by bending the pipe over it. There are various roller supports on the stinger, whose position can be adjusted to achieve controlled bending of pipeline. Once the pipe leaves the stinger, it hangs in the free span between the vessel and the sea floor, known as the *catenary*. Figure 1.2 shows a catenary of a deep water pipelay case. The pipe joint travels through this catenary until it eventually reaches the sea bed. The entire pipeline from the vessel until the seabed makes a S-shaped profile and thereby this method is called the S-lay method of pipeline installation.

The pipeline catenary hanging off from the vessel is held in place by the *tensioners*, which are located after the welding stations. Figure 1.3 shows an example tensioner. These tensioners clamp onto the pipeline surface by means of friction. They act along with the vessel positioning system to maintain required tension in the pipeline.

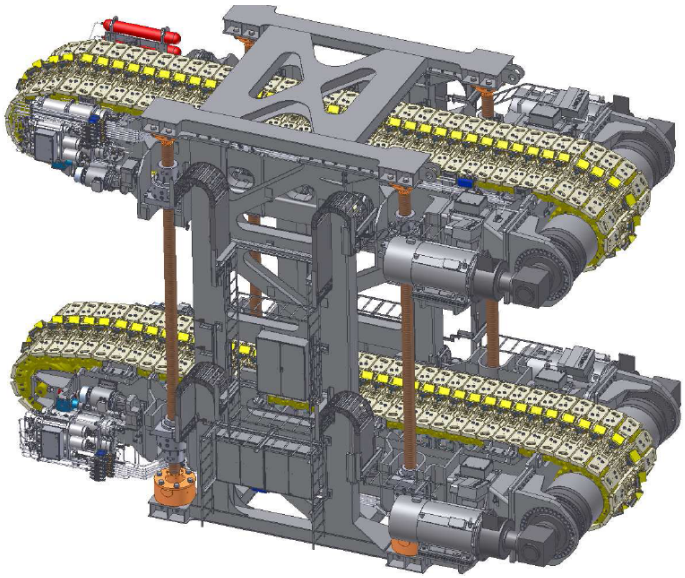

Figure 1.3: Tensioner

Between the tensioner and seabed, the pipeline catenary can be divided into two parts, namely

the *overbend* and the *sagbend*.

Overbend is the part of the catenary that is bent over the stinger. This bending is governed by the position and orientation of the roller supports on the stinger. They ensure that the pipe is not overstressed due to bending. Since the deflection of the pipeline in this region is governed by the position of the supports, it is said to be a *displacement controlled* situation.

Sagbend is the part of the catenary right after the stinger tip, until the point where the pipeline comes in contact with the seabed (known as the *touchdown point* of the pipeline). Since this part of the pipeline hangs freely from the vessel, its configuration is governed by the various static and dynamic loads acting on it. It is therefore said to be a *load controlled* situation. The loads acting on the sagbend are uncontrolled and are therefore crucial to the integrity of the pipeline.

Pipeline integrity must be guaranteed throughout the journey of the pipe from the firing line, through the overbend and sagbend regions of catenary, and after installation (until the end of its operational lifetime).

1.3. Waves and Vessel motions

Since the thesis study is focused around the motions of the vessel in waves, this section will quickly discuss the theory of waves and how vessel response is derived from these waves.

1.3.1. Wave theory

The source of waves in the ocean is the wind which constantly blows over the water surface, transferring its energy to the water in the form of waves. These waves travel over large distances, depending on the amount of energy given to it. Waves cause the sea surface elevation to rise and fall in an irregular fashion.

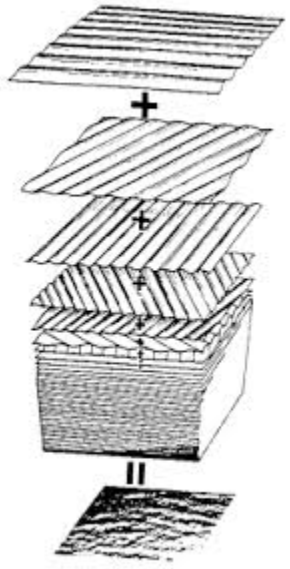

Figure 1.4: Decomposition of irregular waves (Pierson, Neumann and James, 1955)

Although waves are highly complex in nature, they can be broken down into a summation of regular harmonic waves of different frequencies and directions, each with a constant wave

amplitude. (Figure 1.4). There are two kinds of waves based on their origin. Waves that occur due to local wind in the area is often dominated by high-frequency/short-period waves and are known as *wind-sea*. Alternatively, waves which originate from a far away storm and travel large distances to reach the current location are often low-frequency in nature, known as *swell* waves.

Thus, irregular waves can be represented in the form of a spectrum of wave frequencies, with a certain distribution of energy among them. There are many standard wave spectra that have been developed for design purposes. Figure 1.5 shows an example of a uni-directional spectrum, with different frequencies and a energy distribution governed by the JONSWAP spectrum[1]. Other standard spectra include Pierson-Moskovitz, Bertschneider, Ochi-hubble, ISSC etc.,. There are cases where wind-sea and swell waves are present together, acting from two different directions. Such a kind of spectrum has two energy peaks, one due to wind-sea and one due to swell. These various spectral representations of the sea-conditions are vital to determine the dynamic response of the vessel in sea. A detailed information on wave theory can be found in literature[3].

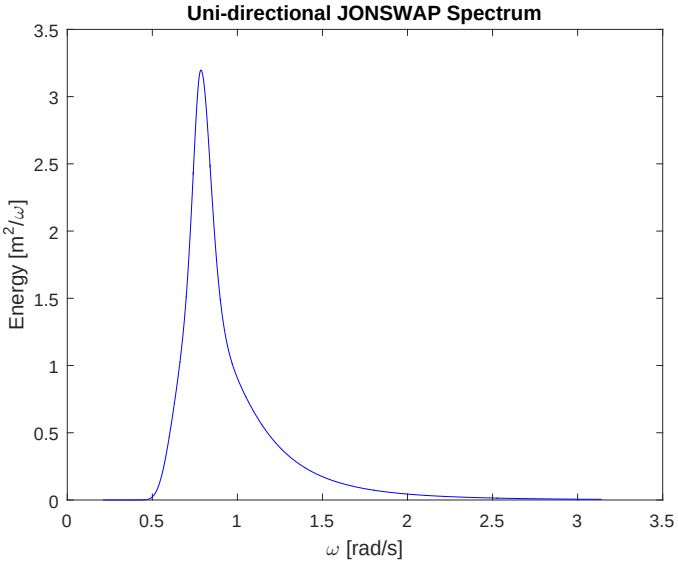

Figure 1.5: Uni-directional wave spectrum example - JONSWAP spectrum

1.3.2. Vessel motions

- The vessel, in general, has 6 degrees of freedom at the centre of gravity, i.e. 3 translations (surge, sway, heave) and 3 rotations (roll, pitch, yaw), also shown in Figure 1.2.
- The vessel motions in surface waves can be defined by the displacement response amplitude operators (RAOs). These RAOs are derived from diffraction analysis, which is detailed in literature[5].
- Each displacement RAO consists of a pair of numbers that define the vessel response to one particular degree of freedom, for one particular wave direction and period.
- Of the two numbers, one refers to an amplitude component which relates the amplitude of vessel motion with respect to the wave amplitude, and the other is a phase component

[1]JONSWAP is a standard spectra that represents the general wave conditions in the North sea

which defines the timing of vessel motion relative to the wave. Figure 1.6 gives an illustration of the vessel motions are derived from wave spectra, using RAOs.

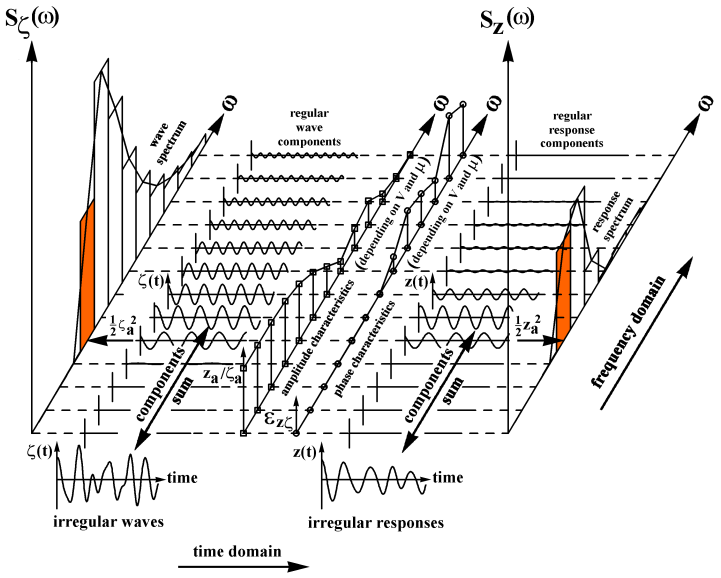

Figure 1.6: Waves and Vessel motions

- In order to arrive at vessel motions, the wave spectrum is discretized into individual components, each with a certain amplitude (the orange box on the left of figure 1.6). The phase between frequency components is randomized. The various frequencies can be summed up to obtain the irregular sea-elevation.
- Once the individual wave components are available, the amplitude and phase are multiplied with their respective RAO values (spectrum shown in centre of figure) to obtain the amplitude and phase of the motion components (right side of the figure). These are then summed up to arrive at the irregular vessel motion time series.

1.4. Thesis outline

1.4.1. Problem background

During pipeline installation, the vessel moves in waves, thereby displacing the pipeline suspended from it. As the weather becomes rough, the amplitude of irregular sea-elevation increases, causing the vessel also to move with a higher amplitude. The pipeline in the sagbend region experiences very high loads due to this motion, most dominating of which is bending loads and axial tension. Beyond a point, the pipeline buckles due to over-stressing. This makes the pipeline unfit for operational use and results in a costly replacement of the respective pipe section.

In order to avoid this buckling phenomenon, the pipeline is abandoned at a point when the vessel motions are too high. The pipeline is placed on the sea-floor, and the vessel either waits or moves away from that location, depending on the severity of the weather condition. Once the weather improves, the vessel picks up the pipeline and continues installation. This entire process is called *Abandonment and Recovery* (A&R) operation.

In order to estimate this point of abandonment, it is important to know the response of the pipe under given loads. Computerized model simulations are used to predict pipe response

for vessel motions occurring in a given sea-environment. These computer simulations are time consuming and therefore cannot be used in real-time to facilitate decision making process offshore. Therefore this point of abandonment is outlined as a criteria during the project preparation phase, often months in advance. Offshore personnel use this criteria to make a decision for A&R operations.

The criteria for A&R operations is formulated in the preparatory phase but the weather in the coming few months cannot be predicted accurately, thereby resulting in many possible load combinations that may occur during installation. In order to overcome this, standardised, unidirectional wave spectra (Section 1.3.1) are used, which represent the most likely occurring sea environment at a particular location. Each of these spectra can have different distributions of energy between the frequencies, depending on the severity of weather condition. In general, a wave spectrum is characterised by the following three parameters:

1. Significant wave height, H_S
2. Zero-crossing period, T_Z
3. Wave encounter angle on the vessel, θ

H_S is the wave height corresponding to the highest $1/3^{rd}$ of the waves, T_z is the average period of the irregular waves and θ is the wave encounter direction on the vessel. Figure 1.5 gives an example of a JONSWAP spectrum with a H_S of 3 meter, T_z of 8 seconds, for a wave travelling in any single direction θ. Various extreme combinations of these parameters are used as input for analysis, the result of which is outlined as an A&R criteria.

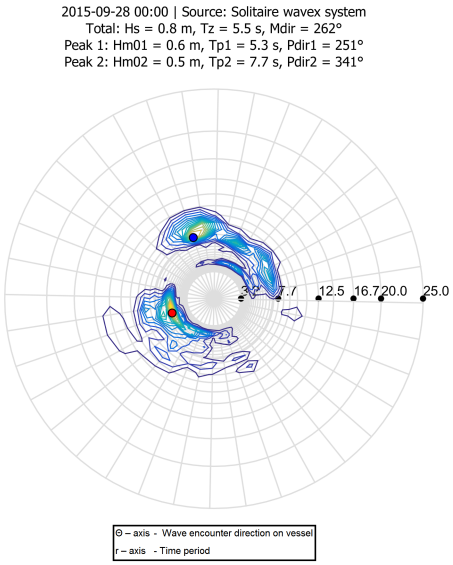

Figure 1.7: Forecast spectrum example

However, this criteria which is obtained based on design sea-spectra is often not optimized for offshore purposes. This is because the sea-state that occurs offshore is much more complex than a simple spectrum represented by three parameters. Figure 1.7 shows an example offshore spectrum, as measured by weather stations around the particular location. The energy distribution does not follow any standard shape and there are multiple spectral peaks in reality. The direction of the waves is also highly spread out, thus making the presently outlined criteria invalid. This then results in offshore personnel taking a decision based on intuition, referring

to the standardised criteria and extrapolating from past experience. The outcome of such a decision making process is often over-conservative, resulting in a loss of valuable vessel time.

Therefore, a criteria is required to outline A&R operations, that is insensitive to sea state definition. Such a criteria should be able to precisely predict the point of abandonment for any given weather condition. This can be achieved by overriding the sea-state parameters as an input for the criteria. The solution will then be to use the *vessel motions* as input, instead of sea-state. This way, there will be no room for uncertainty in decision making process, as the integrity can be assessed for any given vessel motion data, regardless of what kind of sea causes these motions.

1.4.2. Objective

The objective of this thesis is to define a *vessel motion* based criteria for pipeline A&R operations, with respect to pipeline integrity. The aim of developing this criteria is to accurately predict the response of the pipe in the sagbend region, for given motions of the vessel in sea. These predictions will then be used to quickly assess the integrity of pipeline for the given environment, thus facilitating timely abandonment and recovery operations.

1.4.3. Method of approach

This document begins with a detailed description of the mechanics of pipeline installation along with the various modelling aspects (Chapter 2). Chapter 3 describes the general procedure developed during this study, which results in three statistical models to predict the extreme pipeline response in the sagbend. This is followed by the results of the procedure for two sample installation cases, along with its validation (Chapter 4). Finally, the results are analysed and discussed in chapter 5.

Throughout the study, `Orcaflex` software was used for simulating the pipelay model and `Matlab` software was used for further post-processing and analysis.

2

Pipelay Mechanics

This chapter describes the mechanics of the pipeline installation process. The first section describes the pipeline configuration along with the parameters that influence it. Further, a short introduction is given, of the mathematical models that were developed to represent the behaviour of the pipeline catenary between the stinger and the sea bed. The dynamics of the pipelay system is then explained, with an elaboration on the effect of vessel motion on pipeline dynamics. Since Orcaflex is used for all the pipelay analysis presented in this thesis, the numerical method adopted by the software is mentioned. Special attention will be given to modelling of the tensioners.

2.1. S-lay Configuration

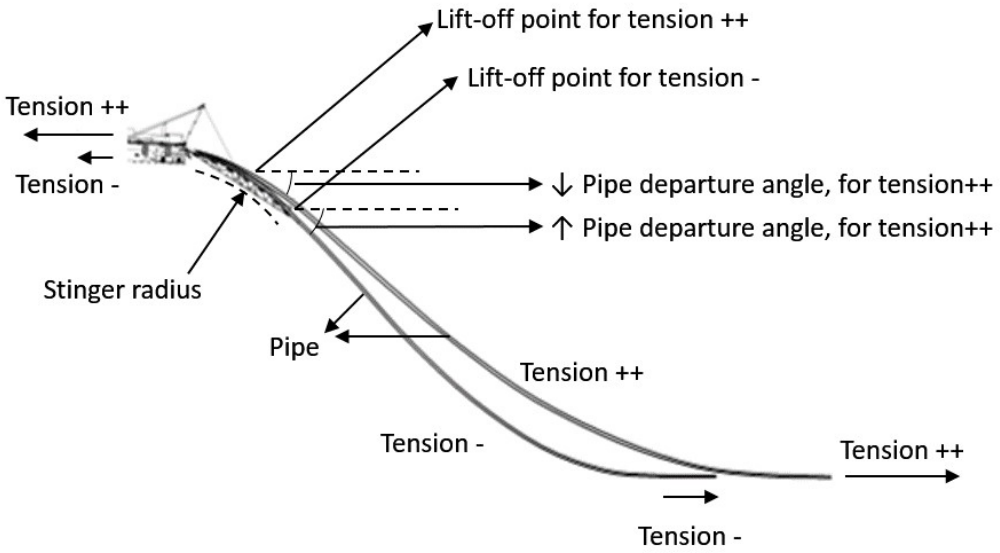

Figure 2.1: Pipeline configuration and influencing parameters

The configuration of the pipeline from the stinger to the seabed is governed by a number of parameters (Figure 2.1):

1. Tension at the vessel
2. Pipe departure angle from the stinger
3. Radius of curvature of the stinger
4. Pipe weight
5. Pipe bending stiffness
6. Water depth

Tension is the force acting in the pipeline axial direction. During installation, tension in the pipeline is provided by the vessel thrusters, which govern the position of the top end of pipeline, relative to the other end which is on the sea bed. The more the vessel pushes forward, the harder it pulls the pipeline, and therefore higher will be the tension. Also, with higher tension, the pipeline that already rests on the seabed is lifted up, thereby moving the touchdown point further away from the vessel. This implies that the vessel has to carry more weight of the pipeline. Tension in the pipeline alters the configuration of the catenary. High tension makes the pipeline catenary straighter and reduces the bending moments, whereas low tension increases bending of pipe near the ends. When the tension is lowered beyond a point, the pipeline buckles due to excessive bending, which is undesirable. Figure 2.1 shows the effect of tension on the pipeline configuration.

Often, it is required to maintain an optimal tension in the pipeline. The tension should be high enough such that the pipe does not buckle. In the same time, very high tension increases the fuel consumption of the vessel.

Pipe departure angle is the angle of the pipe with respect to the horizontal, at the point where the pipe lifts off from the stinger. This angle is crucial in determining how smoothly the pipe leaves the vessel, given a certain tension near the vessel (top tension). A low top tension and a small departure angle tends to bend the pipe downwards immediately after lift-off, thereby increasing the possibility of pipe buckling in that region due to an abrupt change in pipe curvature. Usually the departure angle is governed by the top tension and stinger properties, which are safely designed to meet the integrity requirements of the pipeline.

Stinger radius determines the amount of bending in pipe, in the overbend. A small stinger radius implies that pipe leaves the vessel almost vertically, thereby reducing the free span of the pipeline catenary and also reduces the requirement for high top-tension. However, the strains in the pipe will increase due to increased bending. The stinger radius is usually chosen based on the water depth of installation and the acceptable bending limits of the given pipeline[1].

Pipe properties such as the weight and bending stiffness are usually determined during the design phase of the project, in order to meet the operational requirements of the pipeline. Once these properties are designed, the above installation parameters are chosen accordingly.

The pipe diameter properties determine the allowable radius of stinger. This, in combination with the departure angle, determines the required length of the stinger. Another important

[1] It also depends on the tensioner capacity of the vessel, but recent technological advancements have almost removed such a limitation

parameter in pipelay is the submerged weight of the pipeline. For a given suspended length of the pipe, the submerged weight determines the top-tension of the pipeline.

Water Depth is an important parameter which affects the pipeline configuration. Water depth governs the amount of suspended pipe and therefore affects the design of other installation parameters such as tension and stinger characteristics. Water depth also influences the design of pipe properties. Increased water depth results in an increased external pressure on the pipeline, which means that a larger wall thickness is required in order to withstand the increased pressure.

It must be noted that a change in one parameter affects the influence of the other parameters on the configuration of the catenary. The design of the installation process usually results in calculating the optimal top-tension and stinger characteristics, for a given water depth and pipe properties. Due to the interrelationship between installation parameters, Allseas employs certain criteria for the static design of these parameters, in order to guarantee pipeline integrity.

An example design criteria for static installation case is given below:

1. The maximum overbend *von Mises strain*[2] should not exceed 0.25% and the respective sagbend strain should not exceed 0.15%. These are based on international standards [5].
2. The minimum *bottom tension* should be atleast 6 mT in case of Solitaire
3. The *tip separation* should be at least 0.3 meters in the static case. This is to prevent clashing of the pipe and stinger tip, thereby preventing uncontrolled on the pipe and stinger.

Once the parameters are designed for the static case, dynamics simulations are run using these parameters, to ensure that the chosen values preserve the integrity of pipe in a given dynamical environment. This environment is defined by the wind and wave conditions that impose various loads on the vessel as well as the pipe.

2.2. Mathematical modelling

The previous section described the various parameters that influence the catenary configuration and also stated the design criteria for the static case. In order to design such parameters, we need to assess its influence on the catenary. Dynamic analysis also requires the study of the pipeline catenary, for time-varying loads due to the environment. This is done by various mathematical and finite element models of the pipelay system. This section briefly introduces the various mathematical models that have been developed to reproduce the behaviour of the pipeline between the vessel and the seabed.

There are mainly four methods that are used to model this pipeline behaviour:

1. Natural catenary method
2. Stiffened catenary method
3. Linear beam method
4. Non-linear beam method

[2]Please refer Appendix A for definition of terminology

Natural catenary method models the pipe element as a string with no bending stiffness, which is loaded by its own weight. The advantage of such a formulation is that a very simple and quick analytical solution can be derived. But, the method is inaccurate near the boundaries. It also does not account for the dynamic loads acting on the pipeline. It is however a good approximation of the geometry of a stiff pipe in the sagbend region, given that the axial tension dominates the bending stiffness. The resulting catenary shape is can be given by the following equation:

$$z(x) = \frac{H}{w}\left(\cosh\left(\frac{xw_s}{H}\right) - 1\right)$$

Where $z(x)$ is the vertical position of the pipe for a given horizontal position x, H is the horizontal tension and w and w_s are the dry and submerged weight of the pipeline. A detailed derivation can be found in literature[4].

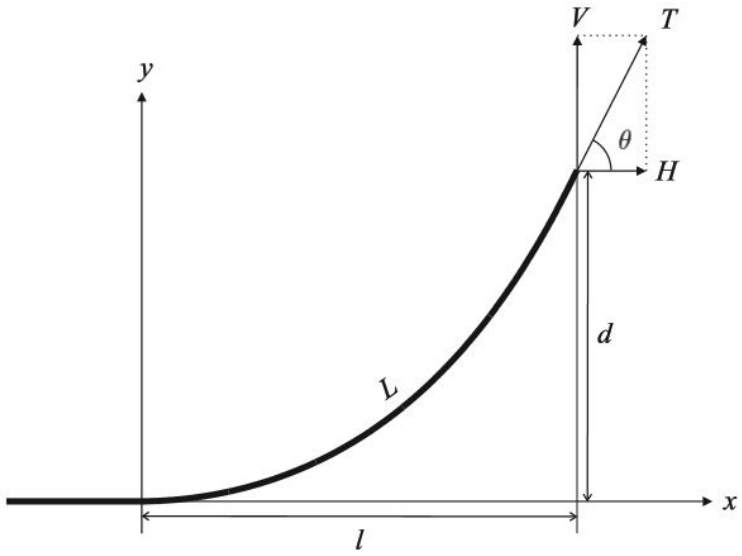

Figure 2.2: Natural catenary description

Stiffened catenary method is an extension of the natural catenary method with the inclusion of a (relatively small) bending stiffness. The solution is also accurately described near the boundaries. Although it can describe the entire pipeline section, the method assumes small bending stiffness of pipeline and therefore is limited to deep water pipelay operations.

The catenary method, although simple, lacks the dynamic behaviour of the pipeline. The reason it is mentioned here is because it is used by the Orcaflex pipelay model to solve the initial statics, highlighting the importance of the catenary equations as an initial step for more advanced models.

Linear beam method employs the linear beam theory and is limited by small pipeline slopes. It is therefore applicable to shallow water pipelay, where the pipe departure angle is near horizontal and the curvature of the pipeline is low. The bending equation of the beam is given by the following expression:

$$EI_b\frac{d^4w}{dx^4} - T\frac{d^2w}{dx^2} - w_s = 0$$

Where EI_b is the bending stiffness of the pipeline. A detailed derivation of this equation can be found in literature[9].

Non-linear beam method assumes the pipeline as a continuous non-linear beam with large deflections. It is applicable for both small and large pipeline slopes and is therefore applicable in shallow and deep water pipelay. The bending equation is given as follows:

$$EI_b \frac{d}{ds}\left(\sec(\theta) \frac{d^2\theta}{ds^2} \right) - T_h \sec^2(\theta) \frac{d\theta}{ds} + w_s = 0$$

Where, s is the distance along the span of the pipeline and θ is the angle at any given s.

For *static* pipelay analysis, the following are the governing equations and boundary conditions of the pipeline installation, using the non-linear beam method.

- Governing Equation 1:

$$EI_b \frac{d^3\theta}{ds^3} - T \frac{d\theta}{ds} + w_s \cos(\theta) = 0$$

- Governing Equation 2:

$$\frac{dT}{ds} = w_s \sin(\theta)$$

- Boundary conditions:

$$\theta(0) = 0 \quad , \quad \left.\frac{d\theta}{ds}\right|_{s=0} = 0$$

$$T(0) = T_h \quad , \quad \theta(L) = \theta_o$$

  Where $s = 0$ is the touch down point of the pipeline on the sea bed, $s = L$ is the other end of the suspended pipe near the stinger tip and T_h is the horizontal tension in the pipeline which is equal to the force applied by the thrusters of the vessel in lay-direction.

A detailed derivation of the equation along with the boundary conditions for the static pipelay case is detailed in literature[6].

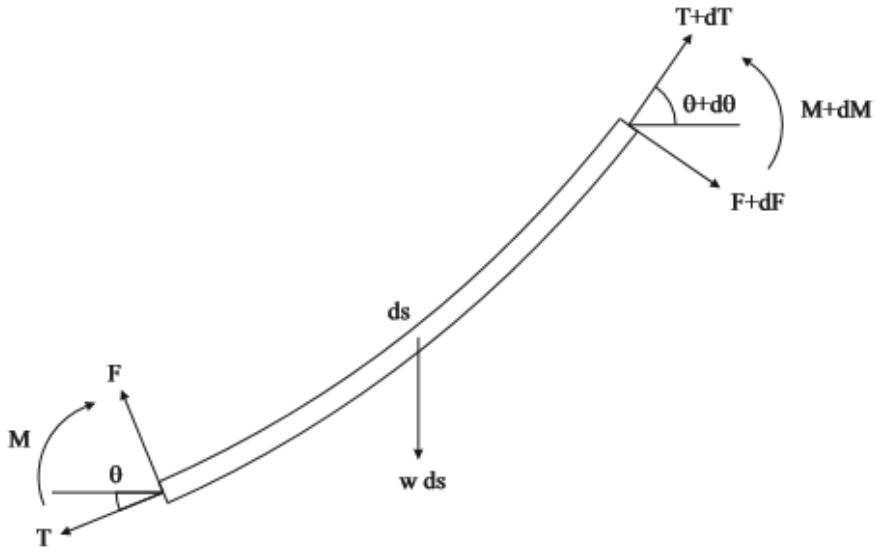

Figure 2.3: Force equilibrium of beam with large deflections

The development of the above methods indicate that the bending stiffness of the pipeline and the boundary conditions of the system are of high importance and therefore need to be modelled accurately. This is because of the fact that the boundary conditions define the amount of suspended weight and tension in the pipeline catenary and the bending stiffness of the pipeline defines the curvature of the pipe near the sagbend, both of which are crucial to determine the integrity of the pipeline.

2.3. Pipelay dynamics

During dynamics, the motions of the vessel in waves cause the above mentioned boundary conditions to change continuously, resulting in a dynamically varying suspended length, suspended weight and tension in the pipeline. Other external forces that act on the pipeline are hydrodynamic loads such as drag, lift, current and wave forces etc. These non-linear forces acting on the dynamical system are modelled in the time-domain, to simulate the accurate response of the pipe at each time step, in the given conditions.

2.3.1. Vessel motions and pipeline integrity

The pipeline ends, between the vessel and the seabed, is not fixed and therefore can change under the influence of environmental conditions. This change is mainly driven by the motions of the vessel, which changes the amount of suspended length in the pipeline. This change in suspended length causes the tension fluctuations in the pipeline. The tension fluctuations from the set value alter the configuration of the pipeline, as decribed in section 2.1.

Thus, the higher the motion amplitudes of the vessel, the higher the tension fluctuations from its design value, and as a result, higher is the likelihood of a pipeline buckle. In order to overcome this dynamic limitation, pipelay vessels are equipped with active tension compensation mechanism, where the tensioners compensate the tension fluctuations by paying-out or hauling-in pipeline. This compensating mechanism alters the suspended length of the pipeline and brings the tension back to its design value. Perfect tension compensation is never achieved during extreme vessel motions, due to various mechanical limitations of the tensioner (such as speed limit of pay-out/haul-in, Maximum pay-out length possible, response lags, etc.,). This calls for an abandonment of the pipeline at a certain stage, when threat to integrity of pipe is imminent. The aim of this thesis is to identify this optimal point of pipeline abandonment, based on vessel motion parameters.

Various researchers have developed dynamical models based on the mathematical models described above, by taking various physical effects into account (Interaction between stinger and vessel, non-linear Pipe stinger interaction, seabed effects, etc.,). Finite element techniques have also been developed to comprehensively model the non-linearities of the system in the time domain. Offpipe and Orcaflex are two such commercial software packages which are considered an industry standard. The next section states the modelling aspects of Orcaflex software.

2.4. Orcaflex model

This section describes the finite element modelling aspects of Orcaflex software for offshore pipelay [2, 8]. The theory of the various topics is briefly stated along with the model details and various interactions between components is discussed.

2.4.1. Waves and vessel motions

- The theory about waves along with their spectral representations are stated in section 1.3.1.

- The irregular wave elevation time history can be extracted from the spectrum of frequencies (Figure 1.5) by discretizing it into components of *equal energy*. Once these individual wave components are obtained, they are combined together with a random phase[3] between them, to obtain the irregular wave elevation.

- The procedure of deriving vessel motions from wave components is listed in section 1.3.2.

2.4.2. Pipeline theory

Pipeline modelling:

- The pipeline is divided into a series of *line segments* which are modelled by straight massless *model segments* having a *node* at each end.

- Each *model segment* only represents axial and torsional properties of the line; and other properties such as mass, weight, buoyancy, drag, etc., are all concentrated to the nodes (arrows in figure 2.4).

- Each *node* is effectively a short straight rod that represents two half-segments on either side of the node. The exception to this is the end nodes, which have only one half-segment next to them and consequently represent just one half-segment.

- Each line segment is divided into two halves and the properties such as mass, weight, buoyancy, drag etc. of each half-segment are lumped and assigned to the node at that end of line segment. Forces and moments are applied to the nodes.

- At the location where a line segment pierces the sea surface, all forces in relation to the fluid are calculated, allowing for varying wetted length up to the instantaneous water surface level.

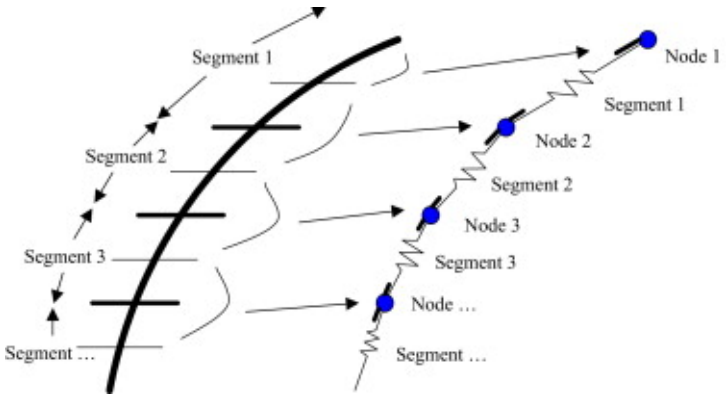

Figure 2.4: Pipeline model - Orcaflex

[3]Phase is the lag between the crests/troughs of two different wave components, defining the timing between them

Structural model:

Figure 2.5 shows the structural model of a single mid-line node and line segments to the either side of it. The figure includes various springs and dampers to model the structural properties of the pipeline, and also shows the local xyz-frames of reference for node and line segment, respectively.

- The axial stiffness and damping of the pipeline are modelled by an axial spring and a damper at the centre of line segment, which applies an equal and opposite effective tension force to the nodes at each end of line segment.
- The bending properties are represented by rotational springs and dampers either side of the node, spanning between axial direction Nz of the node and axial direction Sz of the line segment.
- The torsional stiffness and damping are also modelled by a torsional spring and a damper at the centre of line segment, which applies an equal and opposite torque moment to the nodes at each end of line segment.

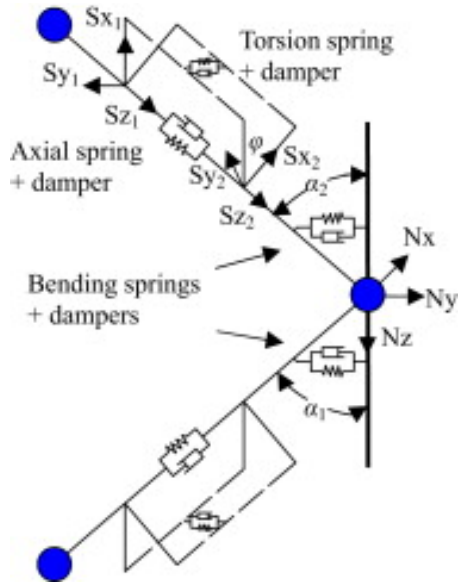

Figure 2.5: Structural pipeline model - Orcaflex

For a detailed list of equations that describe the various internal forces acting on the pipeline, please refer to the Orcaflex theory manual[8].

2.4.3. Interaction models

Pipeline stinger interaction:

The stinger is assumed to be rigidly fixed to the vessel and therefore is assumed to be a part of the vessel. The rollers on the stinger are modelled as fixed supports, given by its position and orientation on the vessel.

Pipeline seabed interaction:

The seabed is modelled as a linear spring with a certain strength defined by the stiffness in the normal direction of the spring.

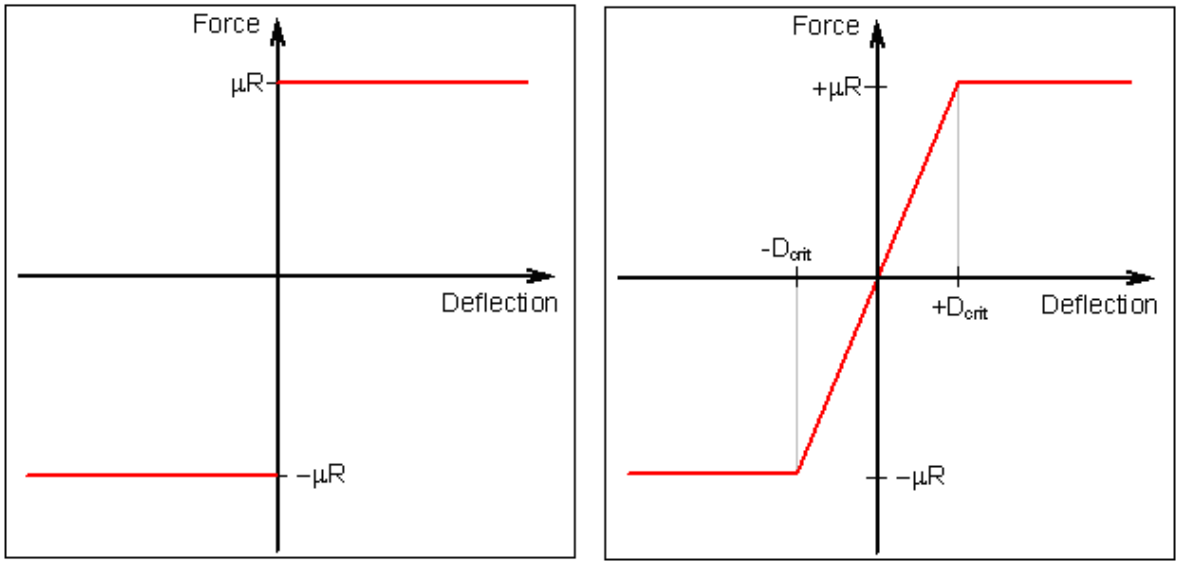

Figure 2.6: Standard Coulomb and modified Coulomb friction models

The seabed friction is a *Coulomb* model in the solid plane whose force equals μR, where μ is the friction coefficient and R is the contact reaction force. Since the resulting curve is discontinuous, it is difficult for a finite element program to solve. Therefore, Orcaflex uses a modified Coulomb model which is illustrated in figure 2.6.

The critical deflection D_{crit} is given by the following formula:

$$D_{crit} = \frac{\mu R}{K_s A}$$

Where K_s is the shear stiffness of soil and A is the contact area.

The next section describes the modelling of tensioners in a detailed manner.

2.5. Tensioner modelling

The tensioner is a crucial part of the modelling process of pipelay as it governs the catenary configuration at each time step. The tensioners on board Solitaire consist of a user programmable control system, which is a P-controller with speed control[10].

2.5.1. Tensioner control system

The P-controller is a feedback loop which minimises the difference in tension using a proportional gain component. A high gain setting means lower deviation from the set tension. This proportional control acts along with a speed control setting which minimises the deviation of the P-controller. Similar to the P-control gain, a high speed setting minimises the control deviations. An additional dead-band setting is used to filter out the small amplitude tension fluctuations which control system need not react to. This dead-band setting however goes to zero during storm conditions, which experiences high tension fluctuations. The control system also has feed forward gain components for heave and pitch velocity of the vessel which help in reducing extreme tension fluctuations, but are almost never used by the operator during Pipelay. Figure 2.7 shows the block diagram of the control system.

Although the control system is programmed to operate in an automatic manner, there is al-

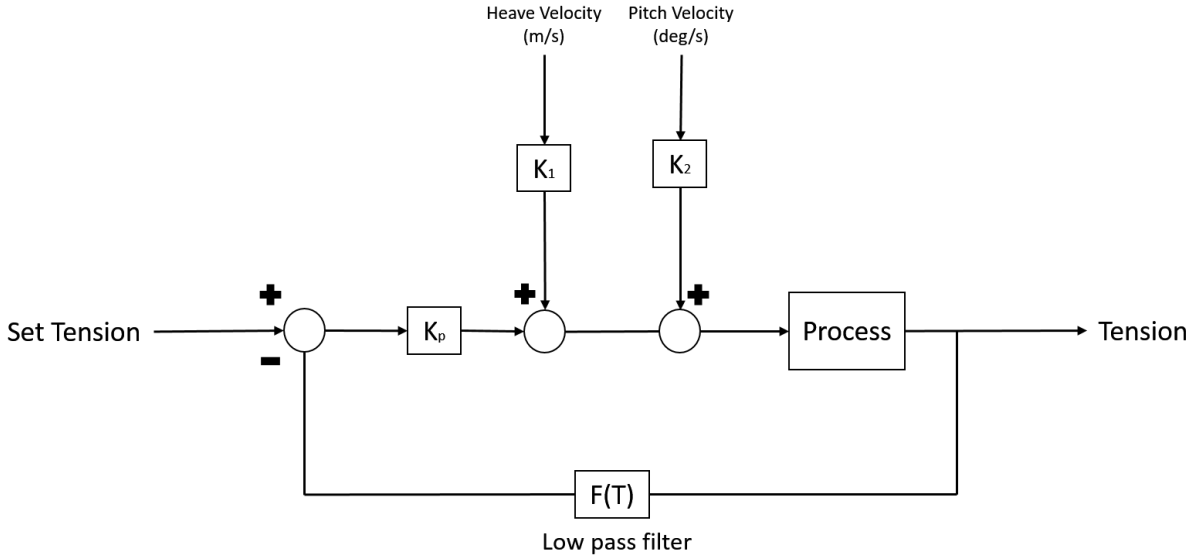

Figure 2.7: Control diagram - Tensioner

ways an experienced controller on board of the vessel to monitor and if required, take over the control of the tensioners during rough weather. The operator, based on experience and intuition, adjusts the gain settings manually according to the requirement. This often results in a dynamic tension which cannot be modelled in a software. However, in order to approximate this behaviour, there are a few methods which have been investigated by Allseas and these are described below.

2.5.2. Tensioner models

There are three tensioner models currently investigated within Allseas, they are briefly described below.

Tensioner dead-band model:

- Allseas is currently using a fully compensating model with a dead-band which corresponds to 20% of the set tension, to account for all inertial effects and delays in the real time system response of the tensioner.
- Dead-band setting allows the tension to fluctuate within the specified limits. Any tension fluctuation that occurs beyond this value is then assumed to be fully compensated by paying-out/hauling-in pipeline (Figure 2.8).
- The dead-band value of 20% is assumed based on historical data. It is derived from the maximum and minimum tension fluctuations that has occurred in past projects (20% of set tension is the most likely value).

Limitations

- The dead-band value of 20% is a generalised consideration, because the tensioner behaviour depends on the sea state occurring in real time as well as type of installation case. For example, in rough weather and with tension compensation, the maximum tension fluctuations may well be above 20%, which is not taken into account by this model.

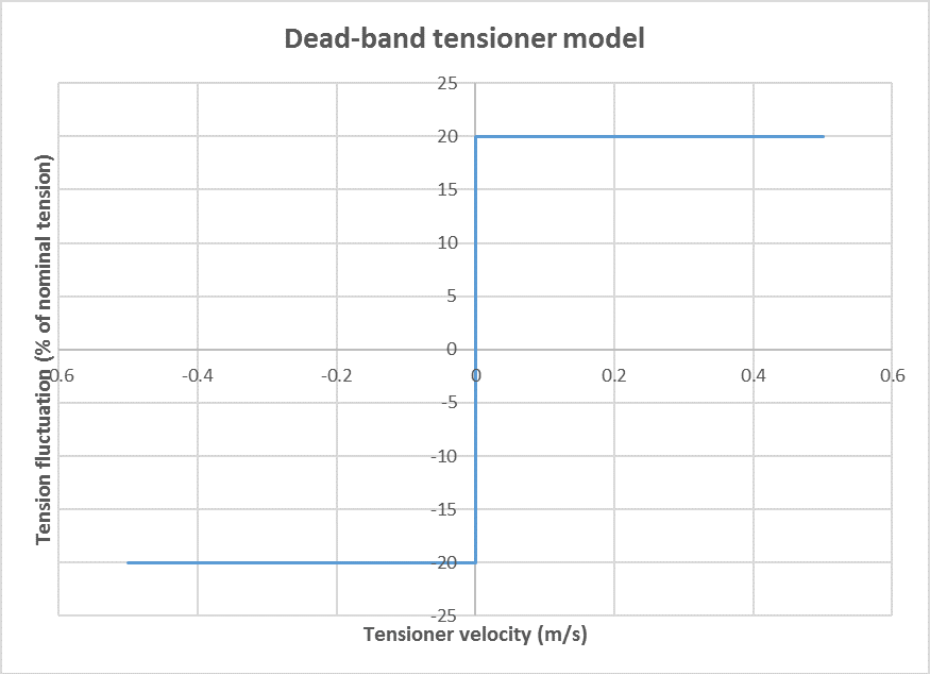

Figure 2.8: Dead-band model of tensioner

- Dead-band implies that once the tension bandwidth has been exceeded, the tensioners are expected to start compensating and maintain the tension within these limits, irrespective of the rate at which they compensate, which is not representative of real tensioner behaviour. The tensioners have a velocity limit for both pay-out and haul-in (0.3 m/s for haul-in and 0.4 m/s for pay-out) which are not taken into account by this model.

Linear damping model:

- This method was developed within Allseas, where the tensioner is modelled as a linear damping element[7].
- The tension outputs resulting from different damping constants were compared to the tension outputs of PIFMS[4] for various installation cases.
- It was concluded that a damping constant of 4000 kN.s/m showed the lowest MAPE[5] and also the least coefficient of variation when compared with the PIFMS data (Figure 2.9).

Limitations

- The damping constant chosen does not account for the velocity limitation of the tensioners as described previously.
- During rough weather conditions, the velocities and accelerations of the vessel are quite high and therefore, the tension operator ramps up the speed setting of the tensioner, for quicker response. Whereas, the linear damping model assumes a monotonously

[4]PIFMS is fatigue monitoring software on board which logs the tension from the load cells on the tensioner
[5]Mean Average Percentage Error

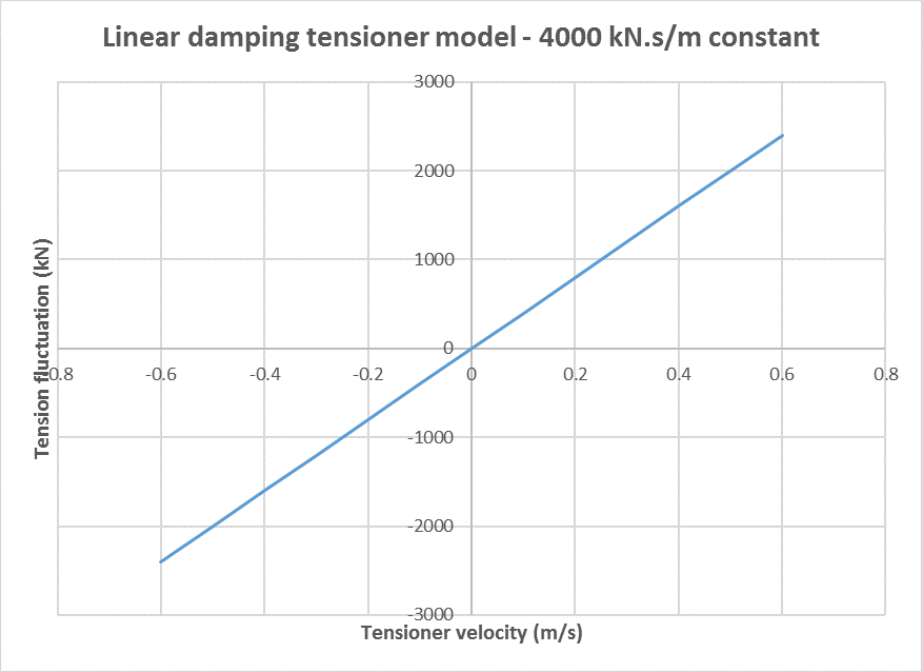

Figure 2.9: Linear damping model of tensioner - $4000kN.s/m$ damping constant

increasing compensation velocity, with respect to increasing tension fluctuations. This therefore does not model the actual behaviour correctly.

Linear damping model with velocity cap:

- This model was proposed during this thesis study, which extends the linear damping model by including the velocity limitation of ±0.3 m/s. Figure 2.10 shows the tension vs velocity curve of this model.
- The motivation for using the damping model is because it is the closest available model approximation of what occurs offshore. The damping model has been validated against real-time tensioner data. This model is more conservative than the dead-band model, as tension values are allowed to attain their maximum peaks, rather than being cut-off with perfect (inappropriate) tension compensation of the dead-band model. This can be seen in figure 2.11.
- Although the velocity limit of pay-out is more than that of haul-in, a constant value of 0.3 m/s is used because the Orcaflex software fails to converge to a solution when asymmetrical damping curve is specified.

Limitations

- Although this model is a step closer to reality, it is still a generalised representation of tensioner behaviour (always assumes a monotonic increase in payout velocity, regardless of the weather conditions).

In order to model the tensioners accurately, other factors should be taken into account such as the maximum length of payout due to workstation limitations, inactivity in calm weather conditions, etc.,. Owing to the conservatism in the other aspects of the design, it is still acceptable

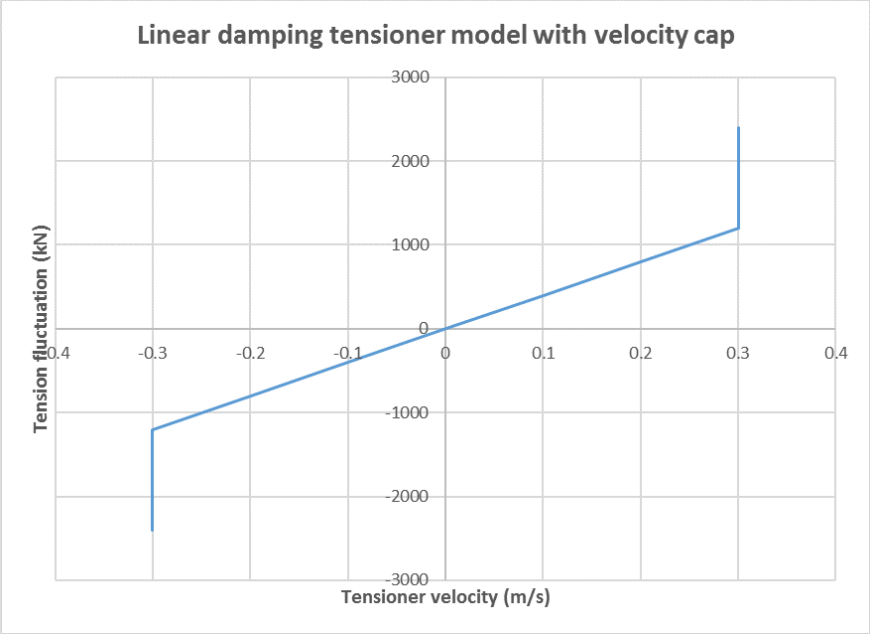

Figure 2.10: Linear damping model with velocity cap

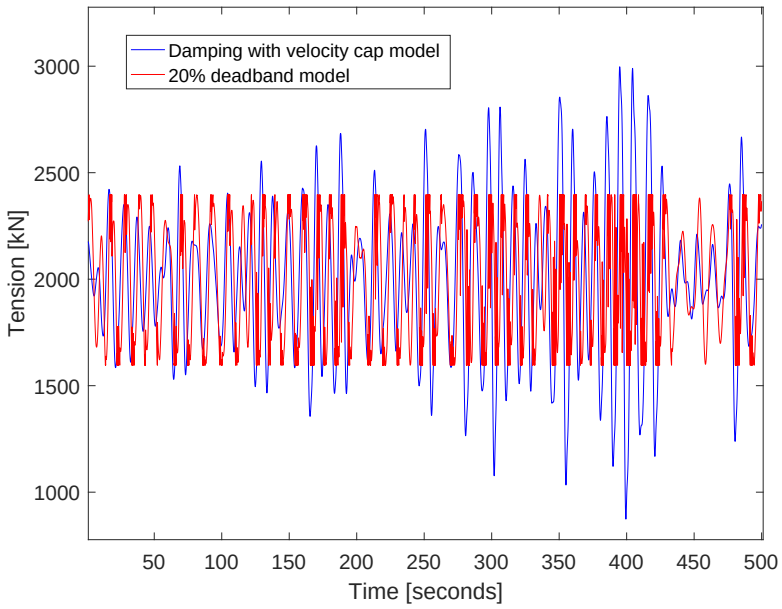

Figure 2.11: Tension output comparison

to use these poor tensioner models project preparation. However, a better tensioner model is recommended while investigating the relationship between tension and vessel motions.

Since study of tensioners is not the main focus of this thesis study, it is assumed that the *damping model with velocity cap* is representative of tensioner behaviour and is therefore used in all further analysis of this thesis study.

3

Procedure

This chapter details the procedure adopted for predicting the extreme responses of pipe, for a given installation case. The first section gives an introduction to the possible methods of approach along with the method adopted in this thesis study. Stated below, are a few pointers that outline the important aspects of the study.

- As per section 1.4.1, this thesis study requires a prediction of extreme responses of pipe for any given environment.
- The predictions need to be for the immediately occurring offshore environment. This is described by the local wind and sea conditions.
- The effect of wind on vessel response is assumed to be small when compared to that of the sea-state. Therefore the wind input is neglected.
- The vessel motions resulting from the multi-directional, non-standard sea-state (see figure 1.6 for example) prediction is assumed to be readily available[1].

Since the entire procedure is based on finding relationships from scatter plots, section 3.2 gives a detailed introduction to scatter plots, along with methods to compare the correlations of different plots. Section 3.4 and 3.5 gives a detailed explanation of the input and output parameter space, on which the data analysis is performed. This is followed by a description of the three different statistical models developed during the study.

3.1. Methods of approach

3.1.1. Frequency domain approach

The initial approach of this thesis study was to look at the input motions and corresponding pipe responses in the frequency domain, in order to explore a relationship between them (RAO's for the pipe response). It was concluded that this method of approach is infeasible due to the following reasons:

- The output pipe response contained new frequencies, which were not a part of the input.

[1]Vessel motion prediction tool developed by the naval department within Allseas

- The amplitude of the various frequencies in the output varied with the amplitude of the input frequencies.
- The above points are the typical characteristics of a non-linear system, which can only be solved accurately in the time domain.
- Attempt on linearising the output results in high error in the maximum value, which is not desired.

3.1.2. Statistical approach

This thesis study employs an *empirical approach* for predicting the extreme response of pipe. This is because of the following reasons:

1. Quick offshore predictions possible when models are fit to data.
2. Interested in *extreme* responses only, and not the process details. Therefore creating a simplified physical model to represent the process is unnecessary.
3. *Accuracy* of the predictions is important to obtain an optimal point for A&R operations. Therefore, finite element models such as Orcaflex are considered as a reliable source of empirical data.

3.2. Scatter plots

Before the procedure is described in detail, an introduction to scatter plots is given in this section, along with the various methods of analysing them.

3.2.1. Introduction

Scatter plot is a graph which plots the data of two variables in the X-Y axis, in order to display a correlation between them. Scatter plots are used for two purposes in this thesis study. The first is to quantify the correlation between an input motion variable and the output variable that represents the integrity of the pipeline. The second purpose is to observe and correct the error in predictions of a given model, by analysing the scatter of the predicted output values against the actual output. For the purpose of generalisation, the following is assumed in this section describing scatter plots:

- X - Input motion variable or Predicted model output
- Y - Output variable or Actual output in error model

The distribution of X and Y gives information on the kind of relation that exists between them. The slope of the scatter shows the direction of correlation that exists between X and Y. A positive slope means that an increase in X corresponds to an increase in Y and vice versa. A zero slope means that the data is uncorrelated. The amount of dispersion present in the scatter describes the strength of correlation. Figure 3.1 shows the various kinds of correlations that exist in a scatter plot. The following sections describe the methods used in this study to analyse input-output correlations.

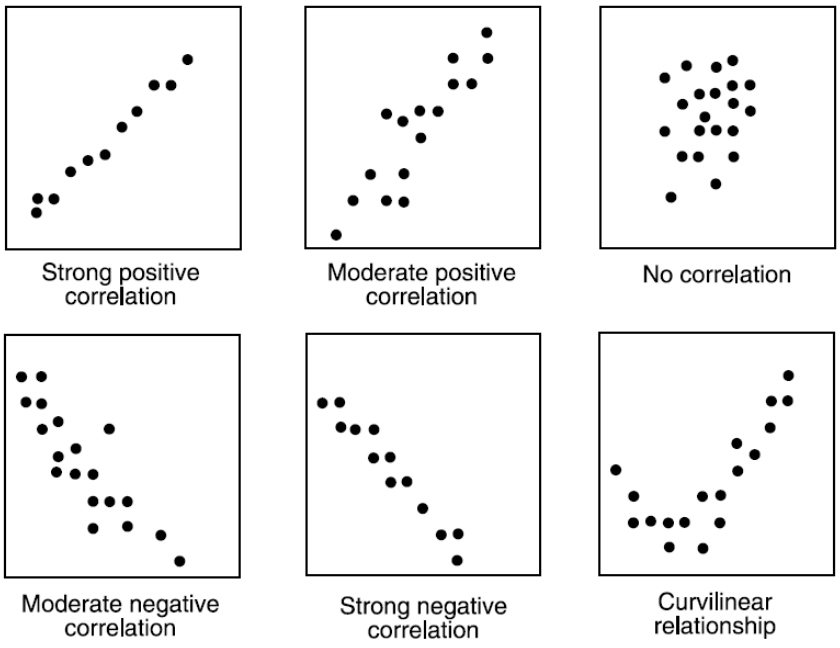

Figure 3.1: Types of correlations in scatter plots

3.2.2. Pearson's correlation coefficient

Pearson's correlation coefficient (Pearson's ρ) gives a measure of linear dependence between X and Y. For N scalar observations of the X and Y, the Pearson's correlation coefficient is given by the formula:

$$\rho(X,Y) = \frac{1}{N-1}\sum_{i=1}^{N}\left(\frac{X_i - \mu_X}{\sigma_X}\right)\left(\frac{Y_i - \mu_Y}{\sigma_Y}\right) \tag{3.1}$$

Where μ_X and σ_X are the mean and standard deviation of X, and respectively, μ_Y and σ_Y are the mean and standard deviation of Y.

ρ can take values between -1 and $+1$, where the magnitude represents the *strength* and the sign represents the *direction* of linear dependency between two variables. Pearson's ρ has been used in certain parts of this thesis study that will be detailed later. It should be noted that Pearson's ρ cannot identify non-linear correlations.

3.2.3. Spread function

In certain cases, it is only required to identify variables that correlate well each other, regardless of the type of correlation that exists between them. In such a case, only the spread of the scatter needs to be quantified to describe their strength of correlation. The more the spread, the more uncertain is the correlation between X and Y. This makes it difficult to make reliable predictions about the data. A lower spread on the other hand means that the data is densely concentrated, thereby increasing the predictability. The following points describe the procedure for quantifying the strength of relationship between the input and the output.

- Figure 3.2 shows a depiction on how the spread is analysed. The dots represents the scatter of each of the N scalar observations of input and the output variables.
- The aim is to find the combination of input and output which shows the best correlation,

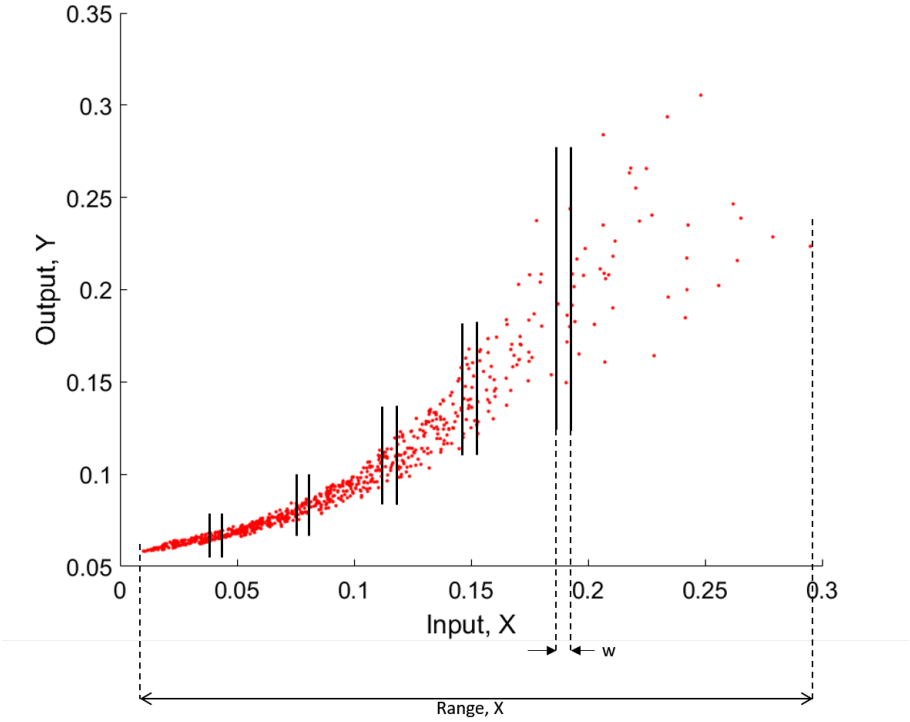

Figure 3.2: Method to determine scatter spread

regardless of the kind of relationship between the variables. This means the spread of output values for a given input should be as low as possible.

- Therefore, the range of input values is split into finite windows, each of small window length, w.
- The windowing length should be small enough to be representative of a unique value in the x-axis and large enough to make sure sufficient number of data points are accounted for, in the population.
- In order to have a general window, regardless of the type of input value, the w is chosen to be 10% of the range of the input values.
- Five windows are chosen along the entire range of the input.
- The spread of values of the output in each window is given by the *coefficient of variation*, which is nothing but the ratio of standard deviation over the mean,

$$S_j = c_v = \frac{\sigma_{Y_j}}{\mu_{Y_j}}$$

Where S_j is the spread of any window j, c_v is the coefficient of variation, μ_{Y_j} and σ_{Y_j} are the mean and standard deviation of the output values belonging to the window j.

- Once the spread S_j is known for all the windows, the overall spread, S of the scatter can be obtained by calculating the mean of the spreads of different windows.

$$S = \mu_{S_j} \tag{3.2}$$

- Since the coefficient of variation is *unitless*, it can be used as a generalized method to compare plots with different kinds of inputs.
- Thus, the strength of relationship of each input-output scatter can be quantified and subsequently, the combination with the least spread can be identified.
- This method is adopted in the procedure of this thesis study, as described in the further sections of this chapter (Section 3.5 - 3.7).

3.3. Database generation

This part involves generating experimental data for different combinations of H_s, T_z and θ (sea-state parameters). The aim of generating this data is to try and reproduce the entire possible range of vessel motions and their respective pipe response, in order to develop a criteria which works for a *generic* vessel motion input. Section 4.1 gives the combinations of sea-state parameters used in this thesis study, along with the justification for its ability to simulate maximal number of vessel motion ranges. The procedure of database generation is described below in steps.

- The installation case details such as pipe properties and water depth are designed for the project requirement and are assumed to be readily available.
- Further, the installation parameters such as stinger configuration, support positions, nominal lay tension, etc., are statically designed using the software *Offpipe*. There are two reasons why Offpipe is used for the static design of an installation case:
  1. The static design requirements developed by Allseas (Section 2.1) has been specifically formulated for the software Offpipe. Also, Offpipe is considered the industry standard for static analysis of pipeline installation [4].
  2. The static design of the installation case is a cumbersome process using Orcaflex. The suspended length of the pipeline as well as the anchor point[2] is required to be specified, which are unknown parameters. Offpipe quickly and automatically calculates these parameters, for a given top-tension.
- The Orcaflex model is now created with the given vessel properties (dimensions, RAOs, etc.), pipe properties and water depth. The static design values such as the support positions, anchor point and pipeline length are transferred from Offpipe to Orcaflex.
- The modelling details of Orcaflex software is given in a Allseas procedural document[12].
- The model dynamics is then simulated for a number of uni-directional JONSWAP sea-states, with different combinations of H_s, T_p and θ.
- For all these cases considered in this thesis study, T_p and θ ranges are constant and are stated in section 4.1.
- The range of H_s however, is chosen according to the installation case. For example, in shallow water pipelay, the maximum operable H_s is much lower than that of a deep water case. This is because of the fact that in deep water, a 2 meter vertical movement of the pipe in the overbend is has a less impact on the pipe response in the sagbend, which is located in a water depth of more than 1000 meters. Whereas the same movement

[2]The anchor point in Orcaflex is the end point of the pipeline on the sea-floor.

becomes crucial for a shallow water case, in a water depth of around 100 meters. For the purpose of generalisation, we will consider the following assumptions:

- R - Total number of simulations, for a given installation case
- N - Total number of data points/time steps in each simulation

3.4. Output Parameter

This section describes the output parameter that is considered in this thesis study. The output parameter should represent the integrity of pipeline during the installation process. It has already been mentioned that the integrity of pipe in the overbend is can be controlled. The integrity of the pipeline is crucial in the sagbend part of the catenary.

Pipeline integrity can be assessed with the help of *buckling checks*[1]. These buckling checks are majorly governed by the *bending moment* and *axial tension* of the pipeline, among other parameters. Bending moment is always an influencing parameter for all installation cases. The importance of axial tension however varies, depending on the installation case. For deep water, the dynamic tension fluctuations are low and therefore its influence on the buckling behaviour is less. The integrity can therefore be represented by the bending behaviour in deep water. The importance of tension however increases for shallow water pipelay, where the tension fluctuations are high and therefore bending alone is not sufficient to represent the integrity of the pipeline. In such a case, *von Mises stress or strain* can be used to represent the integrity of pipeline. This parameter includes the bending and tensile behaviour described previously. It is therefore a better output representation for shallow water pipelay. To summarise, one of the two following parameters can used as the output:

- Bending strain
- von Mises strain

The output variable is only considered for the pipeline node in the catenary, that experiences the maximum dynamic output strain, throughout the whole simulation.

For each simulation, the output variable is recorded for the node with the maximum dynamic output, amongst all the nodes present in the sagbend[3] of the catenary.

The output variable in each simulation can be represented by y_j where j represents any simulation in the database ($j = 1, 2, 3, \cdot, R$). Each simulation contains N number of data points, representing the time history of the output variable in that simulation.

$$Y = y_j(\tau) = \begin{bmatrix} y_1(\tau) & y_2(\tau) & y_3(\tau) & \dots & y_R(\tau) \end{bmatrix}, \qquad j = 1, 2, 3, \dots, R. \quad \tau = 1, 2, 3, \dots, N. \tag{3.3}$$

Where $y_j(\tau)$ is the value of the output variable from the j^{th} simulation, which is a function of the time-step τ.

The design strain value is chosen based on buckling checks on the given pipe and the given installation case. Once the design value is formulated, the output variable should never exceed this design value during dynamics. This means that for any given dynamic scenario, if the maximum strain ever reaches the design value, the pipeline is likely to buckle and therefore this environmental condition is considered unsafe for pipeline installation.

[3] Sagbend of the catenary starts from the pipeline node located just after the stinger tip.

3.5. Input Parameters

Since a vessel motion based criteria is sought after, the input parameters are the vessel motions. The motions are usually given about a reference point, known as the centre of motion. This centre of motion usually coincides with the centre of gravity of the vessel. For all the analysis presented in this thesis study, the reference point is taken at the *stinger tip*[4]. The reason stinger tip is chosen is because this region defines the upper boundary of the suspended pipeline and thereby has a direct influence on the dynamical response of pipeline in the sagbend. Motions can further be characterized by their position, velocity and acceleration.

The input motion components about the stinger tip are listed in table 3.1.

Table 3.1: Input variables

Variable	Description
X_1	In-plane position
X_2	In-plane velocity
X_3	In-plane acceleration
X_4	Out-of-plane position
X_5	Out-of-plane velocity
X_6	Out-of-plane acceleration
X_7	Roll
X_8	Roll velocity
X_9	Roll acceleration
X_{10}	Pitch
X_{11}	Pitch velocity
X_{12}	Pitch acceleration
X_{13}	Yaw
X_{14}	Yaw velocity
X_{15}	Yaw acceleration

Therefore, any given input parameter X_i can be given described by the following equation.

$$X_i = x_{i,j}(\tau), \qquad i = 1, 2, 3, \dots, 15. \quad j = 1, 2, \dots, R. \quad \tau = 1, 2, \dots, N. \tag{3.4}$$

[4]Stinger tip refers to the location of the last roller support present on the stinger

The entire input parameter space can therefore be summarised as per equation 3.5.

$$X = \begin{bmatrix} x_{1,1}(\tau) & x_{1,2}(\tau) & x_{1,3}(\tau) & \dots & x_{1,R}(\tau) \\ x_{2,1}(\tau) & x_{2,2}(\tau) & x_{2,3}(\tau) & \dots & x_{2,R}(\tau) \\ x_{3,1}(\tau) & x_{3,2}(\tau) & x_{3,3}(\tau) & \dots & x_{3,R}(\tau) \\ \vdots & \vdots & \vdots & \ddots & \vdots \\ x_{15,R}(\tau) & x_{15,R}(\tau) & x_{15,R}(\tau) & \dots & x_{15,R}(\tau) \end{bmatrix} \tag{3.5}$$

The motions are defined about 5 degrees of the freedom at the stinger tip. Roll, pitch and yaw are the rotations about the three perpendicular axes of the vessel. The out-of-plane (OP) motions is the same as the sway motions of the vessel. Figure 3.3 gives an illustration of these 4 DOF.

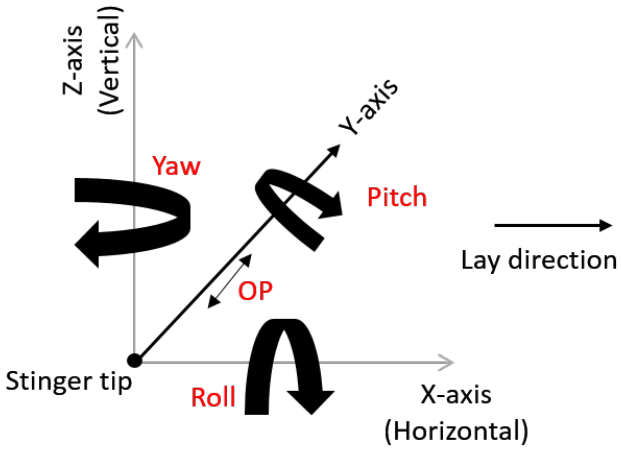

Figure 3.3: In-plane reference direction

The bending of the pipe majorly occurs in-plane (lay direction) and is majorly caused by the motions of the vessel in the same plane (Heave-Surge plane). Unlike vessel motions, in-plane pipe motion need not be referenced about the vertical and horizontal axes, as the pipe orientation along this plane differs throughout the catenary. Since the relation between vessel motions and pipe response is to be identified, it is more convenient to reference the in-plane vessel motions in the direction which has the maximum correlation with the respective pipeline output parameter. Figure 3.4 gives an illustration of the motions about the in-plane reference.

As shown in figure 3.4, θ_{ip} is the angle of the in-plane axis, with respect to the vertical (Z-axis). This angle is chosen based on the direction which shows the maximum correlation between input and output. The correlation can be either between the entire time histories (process) or the extremes. Each of these methods are more likely to result in different angles, since they focus on two different physical aspects of the input-output relationship. These two methods are described in detail, in the following paragraphs.

3.5.1. In-plane angle based on Process correlation method

In this method, the in-plane motions (position, velocity and acceleration) are taken for every angle θ_k present in the second and third quadrant of the X-Z plane ($k = 1, 2, 3, \dots, 180^o$).

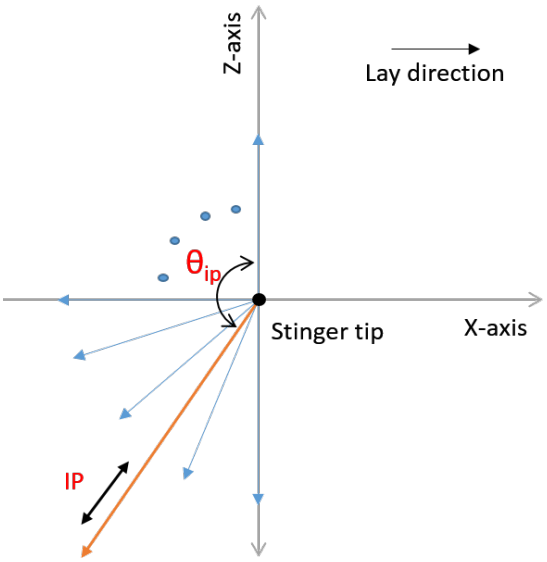

Figure 3.4: vessel motion reference

Equation 3.6 shows the input parameter space for any given angle θ_k.

$$X^{\theta_k} = \begin{bmatrix} x_{1,1}(\tau) & x_{1,2}(\tau) & x_{1,3}(\tau) & \dots & x_{1,R}(\tau) \\ x_{2,1}(\tau) & x_{2,2}(\tau) & x_{2,3}(\tau) & \dots & x_{2,R}(\tau) \\ x_{3,1}(\tau) & x_{3,2}(\tau) & x_{3,3}(\tau) & \dots & x_{3,R}(\tau) \end{bmatrix}^{\theta_k}, \quad k = 1, 2, 3, \dots, 180^o. \tag{3.6}$$

Where each row in X^{θ_k} represents the following:

- $X_1^{\theta_k}$ - Position at angle θ_k
- $X_2^{\theta_k}$ - Velocity at angle θ_k
- $X_3^{\theta_k}$ - Acceleration at angle θ_k

The correlation between the each motion component and the output strain is evaluated using Pearson's correlation coefficient, ρ (Section 3.2.2). Since this is the process correlation method, the correlation is found for the entire time series ($\tau = 1, 2, 3, \dots, N$).The same process repeated for all three motion components.

$$\rho(X_i^{\theta_k}, Y) = \rho(x_{i,j}^{\theta_k}, y_j) = \begin{bmatrix} \rho(x_{1,1}, y_1) & \rho(x_{1,2}, y_2) & \rho(x_{1,3}, y_3) & \dots & \rho(x_{1,R}, y_R) \\ \rho(x_{2,1}, y_1) & \rho(x_{2,2}, y_2) & \rho(x_{2,3}, y_3) & \dots & \rho(x_{2,R}, y_R) \\ \rho(x_{3,1}, y_1) & \rho(x_{3,2}, y_2) & \rho(x_{3,3}, y_3) & \dots & \rho(x_{3,R}, y_R) \end{bmatrix}^{\theta_k} \tag{3.7}$$

Then, the average value of correlation (ρ_{avg}) over R simulations is found for each motion component at a given angle θ_k. Equation 3.8 describes the same.

$$\rho_{avg}(X^{\theta_k}, Y) = \begin{bmatrix} avg\big(\rho(x_{1,1}, y_1), \rho(x_{1,2}, y_2), \rho(x_{1,3}, y_3), \dots, \rho(x_{1,R}, y_R)\big) \\ avg\big(\rho(x_{2,1}, y_1), \rho(x_{2,2}, y_2), \rho(x_{2,3}, y_3), \dots, \rho(x_{2,R}, y_R)\big) \\ avg\big(\rho(x_{3,1}, y_1), \rho(x_{3,2}, y_2), \rho(x_{3,3}, y_3), \dots, \rho(x_{3,R}, y_R)\big) \end{bmatrix}^{\theta_k} \tag{3.8}$$

Finally, the angle corresponding to the maximum of the absolute values of $\rho_{avg}(X^{\theta_k}, Y)$, is chosen for defining the in-plane axis.

$$\theta_{ip} \Rightarrow max\left|\rho_{avg}(X^{\theta_k}, Y)\right|, \quad k = 1, 2, 3, \dots, 180^o. \tag{3.9}$$

Section 5.2.2 gives a detailed analysis of the process correlation method, along with the graphs that show the correlation sensitivity of each input-output combination over different angles θ_k, for the cases considered in this thesis study.

3.5.2. In-plane angle based on Extreme value correlation method

Unlike the process correlation method described above, this method looks at the correlation between extreme values of input and output. The input parameter space is the same as the previous method (Equation 3.6).

The extreme value of a given input time series $x_{i,j}(\tau)$ can be described by the value $x_{i,j}^{q}$, which corresponds to certain probability of exceedance $q\%$.

$$x_{i,j}^{q} \Rightarrow P\left(x_{i,j}(\tau) > x_{i,j}^{q}\right) = q \qquad q = 0, 1, 5, 10\%. \tag{3.10}$$

Therefore, for a given input X_i, the input $P_i^{\theta_k}$ for a given angle θ_k, can be described by the following matrix.

$$PX_i^{\theta_k} = \begin{bmatrix} x_{i,1}^{0\%} & x_{i,2}^{0\%} & x_{i,3}^{0\%} & \dots & x_{i,R}^{0\%} \\ x_{i,1}^{1\%} & x_{i,2}^{1\%} & x_{i,3}^{1\%} & \dots & x_{i,R}^{1\%} \\ x_{i,1}^{5\%} & x_{i,2}^{5\%} & x_{i,3}^{5\%} & \dots & x_{i,R}^{5\%} \\ x_{i,1}^{10\%} & x_{i,2}^{10\%} & x_{i,3}^{10\%} & \dots & x_{i,R}^{10\%} \end{bmatrix}^{\theta_k} \qquad i = 1, 2, 3. \tag{3.11}$$

The correlation between the R extreme values of the input X_i and R extreme values of output Y can be given by spread of Y values over X_i. This is done using the spread quantification method described in section 3.2.3. The q value of 0% refers to the maxima of the time series of a given input variable, with a probability of exceedance of 0%.

$$S\left(PX_i^{\theta_k}, PY\right) = \begin{bmatrix} S\left(x_{i,j}^{0\%}, y_{i,j}^{0\%}\right) \\ S\left(x_{i,j}^{1\%}, y_{i,j}^{1\%}\right) \\ S\left(x_{i,j}^{5\%}, y_{i,j}^{5\%}\right) \\ S\left(x_{i,j}^{10\%}, y_{i,j}^{10\%}\right) \end{bmatrix}^{\theta_k} \qquad j = 1, 2, 3, \dots, R. \tag{3.12}$$

The spread values for different levels of probability of exceedance q are now averaged, in order to obtain an overall correlation of the extreme values of the input and output (Correlation between the tails of the distributions of the input and output).

$$S_{avg}\left(PX_i^{\theta_k}, PY\right) = \frac{S\left(x_{i,j}^{0\%}, y_{i,j}^{0\%}\right) + S\left(x_{i,j}^{1\%}, y_{i,j}^{1\%}\right) + S\left(x_{i,j}^{5\%}, y_{i,j}^{5\%}\right) + S\left(x_{i,j}^{10\%}, y_{i,j}^{10\%}\right)}{4} \tag{3.13}$$

The chosen in-plane angle is the one which has the best correlation. Best correlation in this case refers to the least spread of input-output values.

$$\theta_{ip} \Rightarrow min\left\{S_{avg}\left(PX_i^{\theta_k}, PY\right)\right\} \quad k = 1, 2, 3, \dots, 180^o. \tag{3.14}$$

Section 5.2.2 gives a detailed analysis of this method, along with the graphs showing the correlation sensitivity of each input-output combination, over the different angles θ_k.

The choice of θ_{ip} varies based on the model under consideration. This will be further detailed under each model description (Section 3.6 and 3.7). Therefore, the input parameter space consists of 5 degrees of freedom, each with 3 motion components, resulting in a total of 15 input variables for the parameter space.

3.6. Single input - Single output model (SISO)

The first step in analysis is to check if the strain maxima can be accurately predicted with a *single* motion input variable. The input variable that represents the SISO method is considered to have the most influence on the output extrema, among all other inputs. This procedure to find this input variable is described in the following paragraphs.

In order to define the input parameter space, the in-plane axis needs to defined. Since the SISO model focuses on the extreme value relationship between input and output, the in-plane angle θ_{ip}, is chosen based on *Extreme value correlation method* described in the previous section. The respective motion components about this in-plane axis are taken as inputs for the SISO model.

The input parameter space is given as per equation 3.5 stated previously. There are in total, R number of simulations, each containing N values of the input/output time history (τ). The extrema of this time history $x_{i,j}^{p}$ can be represented by values corresponding to a certain *probability of exceedance*, $p\%$. Note that this is similar to equation 3.10 of the extreme value correlation method.

$$x_{i,j}^{p} \Rightarrow P\left(x_{i,j}(\tau) > x_{i,j}^{p}\right) = p \qquad p = \pm(0, 0.01, 0.05, 0.1, 0.5, 1, 5, 10)\%. \tag{3.15}$$

$$y_{j}^{p} \Rightarrow P\left(y_{j}(\tau) > y_{j}^{p}\right) = p \qquad p = 0, 0.01, 0.05, 0.1, 0.5, 1, 5, 10\%. \tag{3.16}$$

The $\pm$ sign for p in equation 3.15, indicates either the positive extrema (maxima) or the negative extrema (minima) of the input variable based on its overall[5] direction of correlation with the output. For example, an average positive correlation means that the input extrema is taken with a probability of exceedance of 10% and if the direction of correlation is negative, then the corresponding probability of exceedance is 90%. For the output variable however, only the maxima is considered. A 0% probability of exceedance means the maximum value in the entire time history.

Figure 3.5 gives a example visualisation of the various levels corresponding to a certain Probability of exceedance (PE). The motivation to use PE values is because these are a better representation of the extrema of a stochastic process[6].

Now, each input variable X_i^p, with a certain probability of exceedance p is scattered against the output Y^p, with the same probability of exceedance; both variables having R values representing the extrema of R simulations. The spread S, is then quantified for the given scatter.Figure 3.2 and section 3.2.3 give the illustration of the method adopted to quantify the spread in an

[5]The term overall means that the Pearson's correlation coefficient between the input and output time histories is averaged for R simulations. The resulting sign of the average coefficient value is taken as the overall direction of correlation of input with the output.

[6]A stochastic process is one which includes a certain randomness in it's occurrence. Pipelay is one such stochastic process because of the discretization of a continuous wave spectrum with random *phase* between individual harmonics.

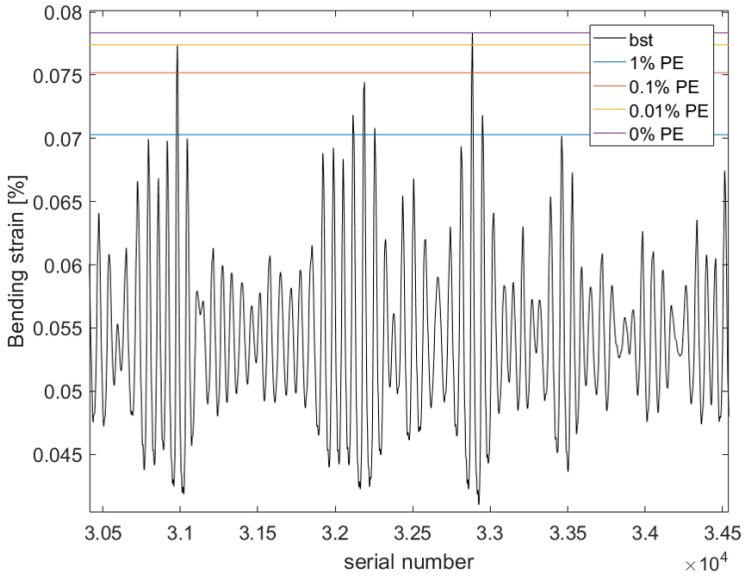

Figure 3.5: Visualisation of Probability of exceedance levels (*bst* - Bending strain time series)

input-output scatter.

$$S_{i,p} = S\left(X_i^p, Y^p\right) \quad p = 0, 0.01, 0.05, 0.1, 0.5, 1, 5, 10\% \tag{3.17}$$

The process is repeated for all p values of probability of exceedance. Out of the various input-output combinations, the one with the least spread is chosen as the best representation of the single input - single output model.

$$S_{min} = min\left(S_{i,p}\right) = min\begin{pmatrix} S_{1,0\%} & S_{1,0.01\%} & S_{1,0.05\%} & \cdots & S_{1,10\%} \\ S_{2,0\%} & S_{2,0.01\%} & S_{2,0.05\%} & \cdots & S_{2,10\%} \\ S_{3,0\%} & S_{3,0.01\%} & S_{3,0.05\%} & \cdots & S_{3,10\%} \\ \vdots & \vdots & \ddots & \vdots & \\ S_{15,0\%} & S_{15,0.01\%} & S_{15,0.05\%} & \cdots & S_{15,10\%} \end{pmatrix} \tag{3.18}$$

This chosen scatter can then be represented mathematically in a formula, which can be derived from best-fit procedures described in section 3.9. This chosen input of the SISO method (corresponding to least spread) is considered to have a maximum influence on the output extrema, among all other inputs. Therefore, this variable is considered to be the *dominating* variable (X_{dom}) in the entire input parameter space. This dominating variable will further be used by the subsequent models. Figure 3.6 summarises the SISO procedure stated in this section.

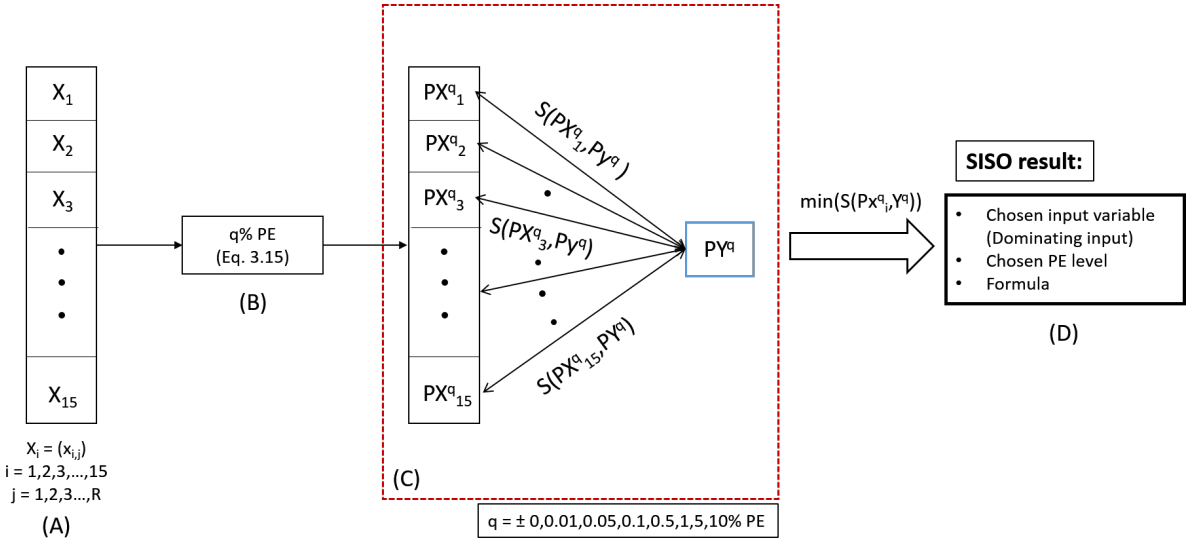

Figure 3.6: Illustration of SISO procedure

3.7. Multiple input, Linear Regression model (MIR)

The multiple input model is used to predict the maximum output values, using more than one input variable.

The in-plane angle for this method varies based on the installation case considered. This is because the physical nature of the process changes for every installation case. In deep water, the system is fairly linear, in the sense that the variation of the TDP with respect to the vessel motions is proportional. Whereas for shallow water pipelay, the non-linearities (TDP variation) of the system are more pronounced, even at lower motion amplitudes of the vessel. This is because of the near horizontal departure angle of the vessel and coupled with the high set tension. Therefore in deep water, the process correlation method, which takes the entirety of the process into account, will lead to the most appropriate choice of θ_{ip}. In shallow water, the extreme value correlation method is more suited to obtain θ_{ip}.

This method can be better explained with an example time series of one output and three inputs, given in figure 3.7. The aim of this method is to predict the maximum output. The (orange) square in the first graph represents the maximum location of the output variable. This location of the maximum output is important to the method, as the input values are recorded around this maximum output location. It is known that the *dominating* variable (SISO output) has the highest influence on the output extrema amongst all other inputs. It is more likely that a maximum of this input variable will cause the output maximum and therefore, the location of this peak should lie close to that of the maximum output. This is also shown in figure where the location of green square (maximum of dominating input variable) is just before the orange square[7]. All the other inputs occurring around the location of this dominating input, is assumed to subsequently influence the output strain maxima.

Therefore, a *window*,w_o, is chosen before the location of the *dominating* variable extrema. This window is chosen based on sensitivity study, which identifies the window with the best predictions (i.e., least spread. This part about spread will be discussed below). It is known the extremes of the input variables cause the output maximum; but the exact input value is unknown. Therefore, within this interval w_o, the input variables $X_i^{p_o}$ corresponding to a certain

[7]The input variables are assumed to have a negative correlation with the output and therefore the minima is shown.

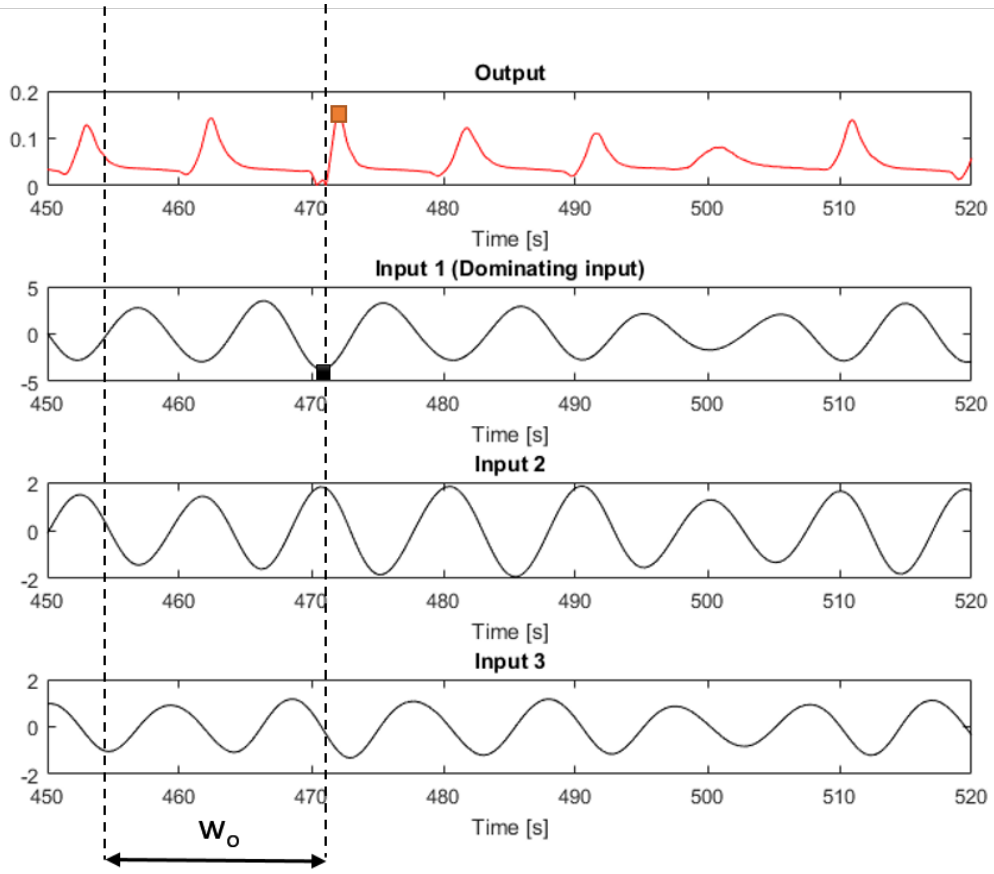

Figure 3.7: Example time histories - MIR method

probability of exceedance p_o, is taken as input for analysis. This is also shown in figure 3.8, for the time history of input 2 from figure 3.7, within the given window w_o.

$$X_i^{p_o} = x_{1,j}^{p_o} \Rightarrow P\left(x_{i,j}(\tau) > x_{i,j}^{p_o}\right)\Big|_{w_o=a}^{b} = p_o\% \tag{3.19}$$

Now that the inputs and the output variables are available, the procedure for analysis is described in the following steps.

- The multiple inputs $X_i^{p_o}$, are combined linearly using the *multiple linear regression* method, which assigns constant coefficients/weights to each input based on the data available.

$$Y_{max,pred} = \sum_{n=1}^{n_o} b_n \cdot X_{n,i}^{p_o} \tag{3.20}$$

  where n_o is the chosen number of inputs for regression analysis, b_n are the regression coefficients/weights assigned to the respective inputs, $Y_{max,pred}$ is the *predicted* output maximum.

- Since there are 15 different motion variables, and n_o number of regression inputs, this results in ${}^{15}C_{n_o}$ possible input combinations. Therefore each of these combinations should be analysed to arrive at a optimal set of input variables.

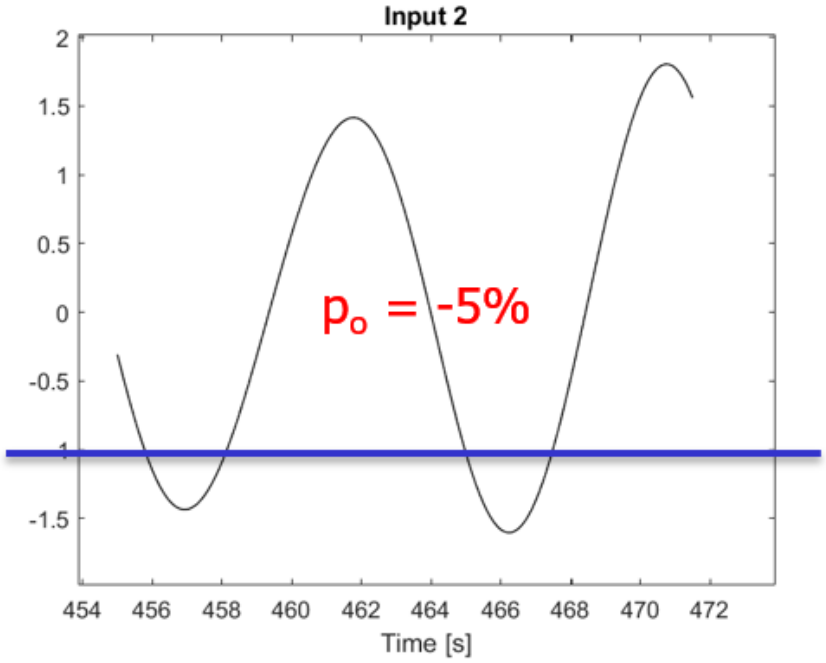

Figure 3.8: Input values for MIR method. Negative probability to represent minima, due to negative correlation with output. Input 2 is only illustrated here, within the given window w_o

- The weights are derived by performing regression analysis on the database, which results in a linear approximation of the output, for a given set of input variables. This linear approximation always gives a certain error e in predictions, when compared to the actual values.

  $$e = Y_{max,actual} - Y_{max,pred}$$

  This error might increase/decrease over the range of predicted values. Also, this variation of e with respect to $Y_{max,pred}$, might be linear/non-linear depending on the combination of input values chosen for regression.

- The error in predictions can be visualised by scattering the predicted values against the actual output derived from simulations. Figure 3.9 shows the different kinds of error scatters.

- Regardless of the type of error function, a mathematical error model can be fit to the data and subsequently incorporated back into the prediction model, to compensate for these errors. The only requirement is that the *spread* S, of the error data should be low. In order to achieve this, various combination of input variables should be tested and the combination with the least spread is chosen.

- Once the final combination is chosen, the error model can be found using best-fit procedures. This results in the following equation:

  $$Y_{max,final} = erf(Y_{max,pred}) \tag{3.21}$$

  where, $erf(Y_{max,pred})$ is the *error function*, which depends on $Y_{max,pred}$ (Equation 3.20).

Section 5.1.2 gives a detailed analysis of the MIR method for the cases considered in this thesis study, along with its advantages and limitations. Figure 3.10 summarises the MIR procedure.

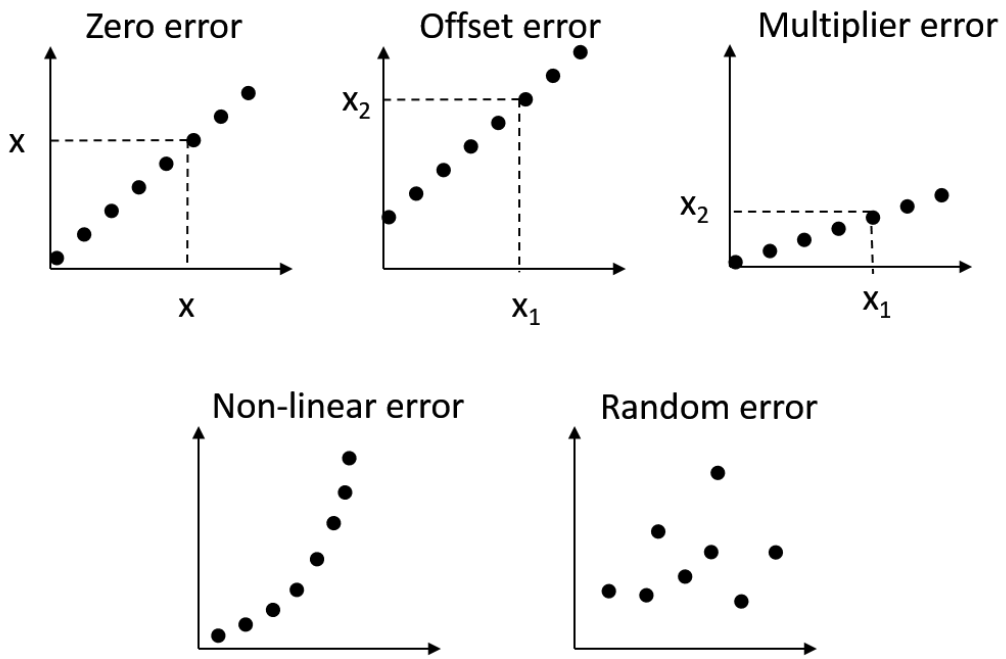

Figure 3.9: Types of error

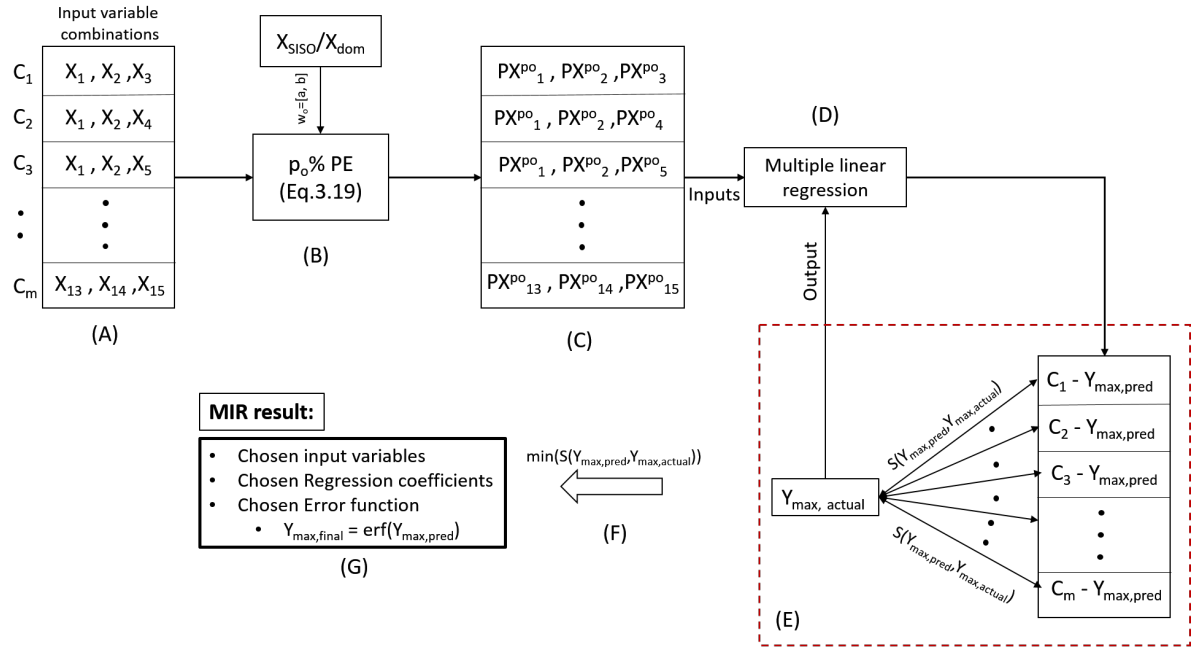

Figure 3.10: Illustration of MIR procedure

3.8. Multiple input, Piecewise-linear, Regression model (MIPR)

This method follows the same procedure as the above method, except that multiple regression is performed for separate groups of the same database. Mutiple regression, in general, is a linear method and therefore the regression coefficients are constant (constant gradient). Pipeline installation on the other hand is a non-linear process, where the non-linearities in the system become more dominant when the motions become larger. The database is generated for low and high strains which are caused by small and large motion amplitudes respectively, and

therefore may contain linear and non-linear combinations of inputs within the same database. Performing linear regression on this database as a whole, will lead to coefficients that are not optimal.

Splitting this database according the range of motion amplitudes will to a fair extent, split the data into groups of similar behaviour. Performing linear regression on these separate groups of data will result in better regression coefficients for each group. The split of data is based on the *dominating* input variable (SISO output, section 3.6). Since this variable has the most dominating influence on the output extrema, any increase in its extreme value is assumed to cause a monotonic increase in the output maxima. This results in groups of data whose output values should not overlap with each other; thereby assuming the split of data into groups of similar behaviour.

The procedure is exactly the same as multiple linear regression, except that it is repeated for different datasets belonging to the same database. In this thesis study, the data is split into two groups along the *median* of the distribution of the dominating input $X_{dom,ext}$. The equations 3.20 and 3.21 now become

$$Y1_{max,pred} = \sum_{n=1}^{n_o} b1_n \cdot X1_{n,i}^{p_o}, \qquad Y1_{max,final} = erf(Y1_{max,pred}) \tag{3.22}$$

$$Y2_{max,pred} = \sum_{n=1}^{n_o} b2_n \cdot X2_{n,i}^{p_o}, \qquad Y2_{max,final} = erf(Y2_{max,pred}) \tag{3.23}$$

It is to be noted that the window w_o and the input probability of exceedance, p_o is chosen based on sensitivity study. However, this sensitivity study is based on the dataset with higher motion amplitudes and its corresponding strain maxima, since this region is of importance to this particular study. Figure 3.11 summarises the procedure of the MIPR method.

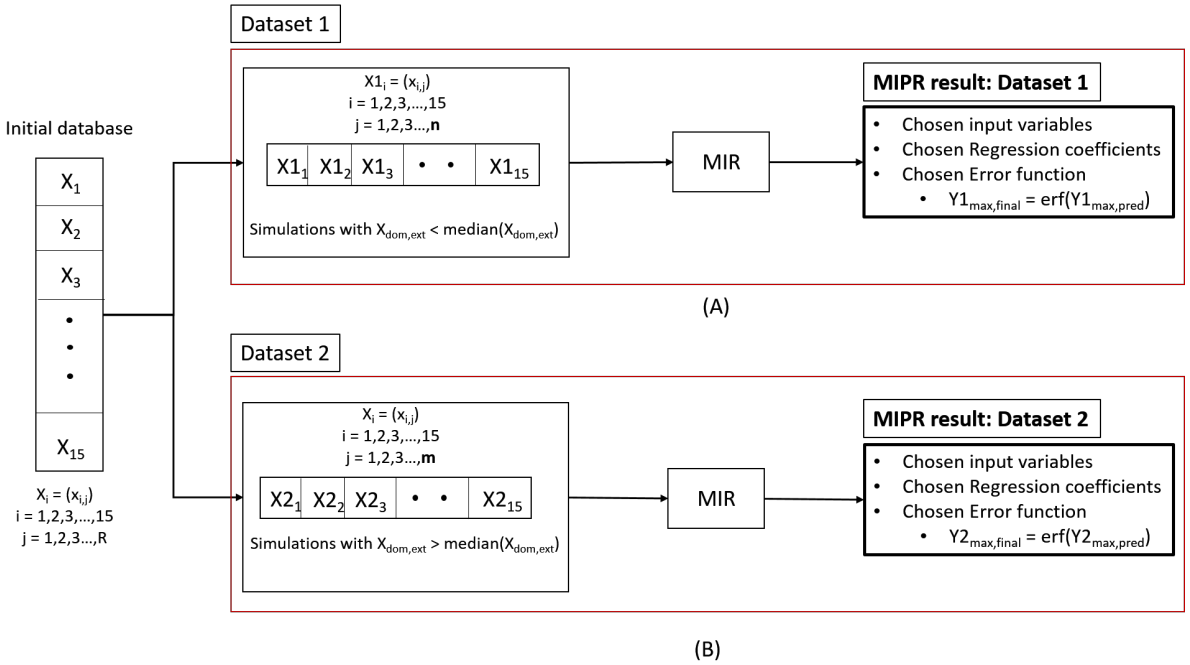

Figure 3.11: Illustration of MIPR procedure

3.9. Curve fitting of scatter plots

The resulting scatter plots from the three statistical models need to be expressed mathematically, in order to make predictions using formulas. Curves are fitted to the scatter plots, using the `fit` function in `Matlab`. All the scatter plots were fitted with three models,

1. First order polynomial (straight line)
2. Second order polynomial
3. Exponential curve

The Root Mean Squared Error (RMSE) was used to compare the goodness of fit of these three models. The model with the least RMSE value is chosen as the best fit of the given scatter.

Figure 3.12 summarises the entire procedure described in this chapter. References are made to the respective section as well as parts of figures, for elaborate explanations.

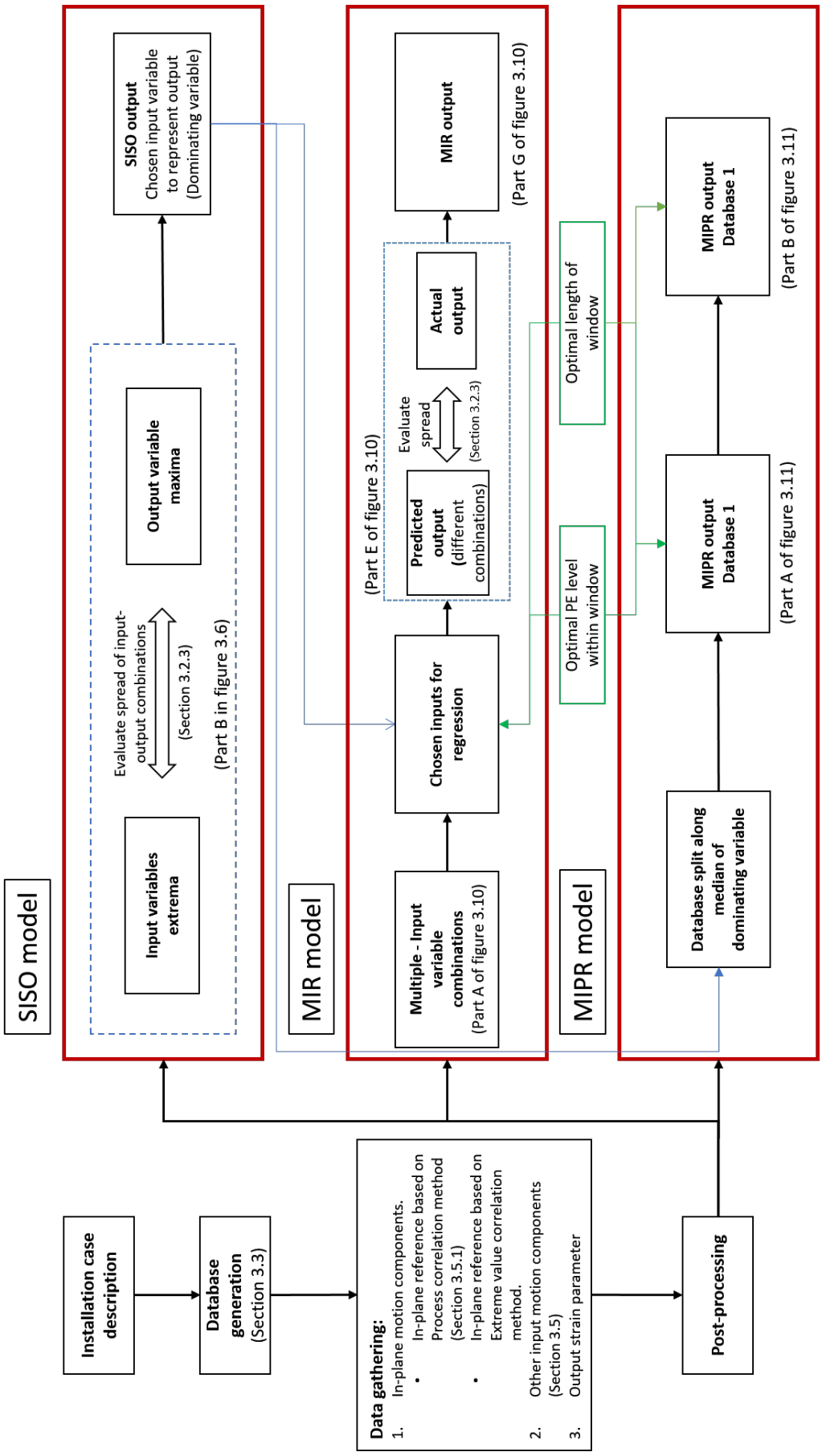

Figure 3.12: Illustration of overall procedure

4

Results & Validation

This chapter presents the results of the procedure stated in chapter 4, for two different installation cases. The first case is a typical deep water installation with a flexible pipe, whereas the second case is in shallow water with a very stiff pipe. The results are then validated for a set of randomly chosen sea conditions, which are not a part of the initial database. These results are analysed further in chapter 5.

4.1. Installation case details

Table 4.1 states the installation parameters of the two cases considered in this thesis study; one in deep water and one in shallow water. The deep water case has a relatively flexible pipe whereas the shallow water installation is with a very stiff pipe. These two extreme cases were chosen to generalise the models under study, for all water depths and pipe properties. The following are the combination of sea-state parameters:

- H_s, Deep water - **1**, 1.5, 2, …, **4** meters.
- H_s, Shallow water - **1**, 1.5, 2, …, **3** meters.
- T_z : **5**, 6, 7, …, **15** seconds.
- θ : **0**, 10, 20,…, **90** degrees.

The sea-states described above are assumed to excite all the possible ranges of vessel motions. These combinations of sea-states simulate the RAO's of the vessel from 0 degrees to 90 degrees which also includes the worst angle for solitaire i.e., 70 degrees. Moreover, the variation of T_z excites all the possible frequencies which have a contributing part in the RAO graphs. Beyond 15 seconds, the energy in the RAO spectrum is small and therefore it is assumed to be sufficient to simulate up-to a 15 second wave period. The wave heights are simulated up-to the design limit of the vessel during pipelay operations (4 meter). The shallow water case is only simulated up-to a 3 meter significant wave height. This is because the system non-linearities are in general higher than the deep water case. Increasing the sea-state beyond 3 meters causes the strains to increase un-proportionally, deteriorating the quality of the data on the whole (not desired).

The database is generated in Orcaflex for both cases. The modelling details of the pipelay system in Orcaflex is described in an Allseas procedural document[12]. Once the database is

Table 4.1: Installation parameters

Parameter	Deep water	Shallow water	Unit
General properties			
Water Depth	1500	122.8	m
Vessel	Solitaire		[-]
Stinger length	140		m
Stinger Radius	120	300	m
Pipe properties			
Outer diameter	20	44	$inch$
Wall thickness	25.4	24.6	mm
Material	X65 Steel		[-]
SMYS	448		N/mm^2
SMTS	530		N/mm^2
Static case parameters			
Top tension	2000	2900	kN
Bottom tension	446	2400	kN
Pipelay Von Mises strain (sagbend)	0.0845	0.064	%
Maximum bending strain (sagbend)	0.055	0.048	%
Dynamic integration parameters			
Integration time step	0.1		$seconds$
Sampling interval	0.1		$seconds$
Simulation time	3600		$seconds$

generated, the input and output variables are recorded for further analysis. The general input parameter space is listed in table 4.1. the in-plane angle (θ_{ip}) varies, depending on the model under consideration. It will be stated separately along with each model's results. Table 4.2 details the general parameters considered for data analysis. The following sections illustrate the results of three statistical models, for the two installation cases considered here.

Table 4.2: General parameters for Data analysis

Parameter	Deep water	Shallow water	Unit
Output variable, Y	Bending strain	von Mises strain	%
Number of simulations, R	770	550	-
Data points per simulation, N	36000		-

4.2. Single input - Single output model (SISO)

4.2.1. Deep water

Table 4.3 details the results for the deep water case. Figure 4.1 shows the respective scatter of the output (black dots) along with the model fit to the data (red line).

Table 4.3: SISO results - Deep water

Parameter	Result
In-plane angle, θ_{ip}	171 $degrees$
Input variable, X_{siso}	In-plane (IP) velocity at stinger tip, X_2
PE, p_{siso}	10%
Formula	$Y^{10\%} = -0.001759 \cdot (X_2^{10\%})^2 + 0.01526 \cdot X_2^{10\%} + 0.05468$
RMSE - model fit	5.36e-04

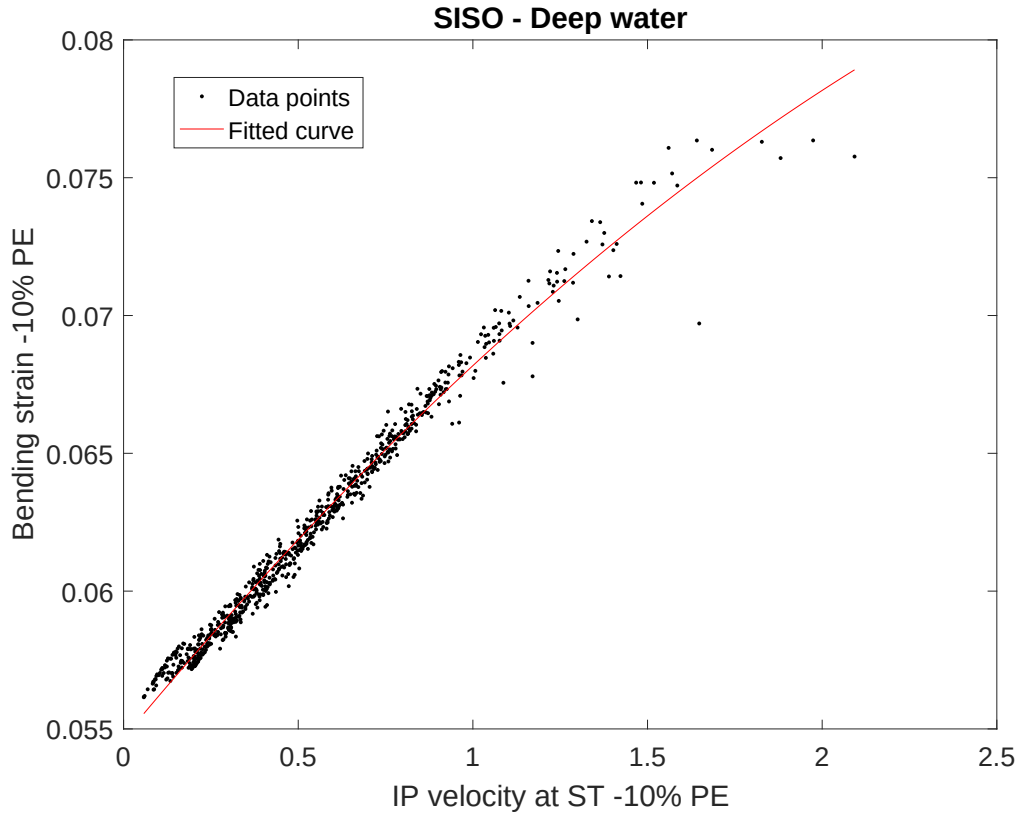

Figure 4.1: SISO - Deep water

4.2.2. Shallow water

Table 4.4 details the results for the shallow water case. Figure 4.2 shows the respective scatter of the output (black dots) along with the model fit to the data (red line).

Table 4.4: SISO results - Shallow water

Parameter	Result
In-plane angle, θ_{ip}	162 $degrees$
Input variable, X	In-plane (IP) acceleration at stinger tip, X_3
PE, p_{siso}	5%
Formula	$Y^{5\%} = 0.006836 \cdot (X_3^{5\%})^2 + -0.005964 \cdot X_3^{5\%} + 0.07231$
RMSE - model fit	0.003

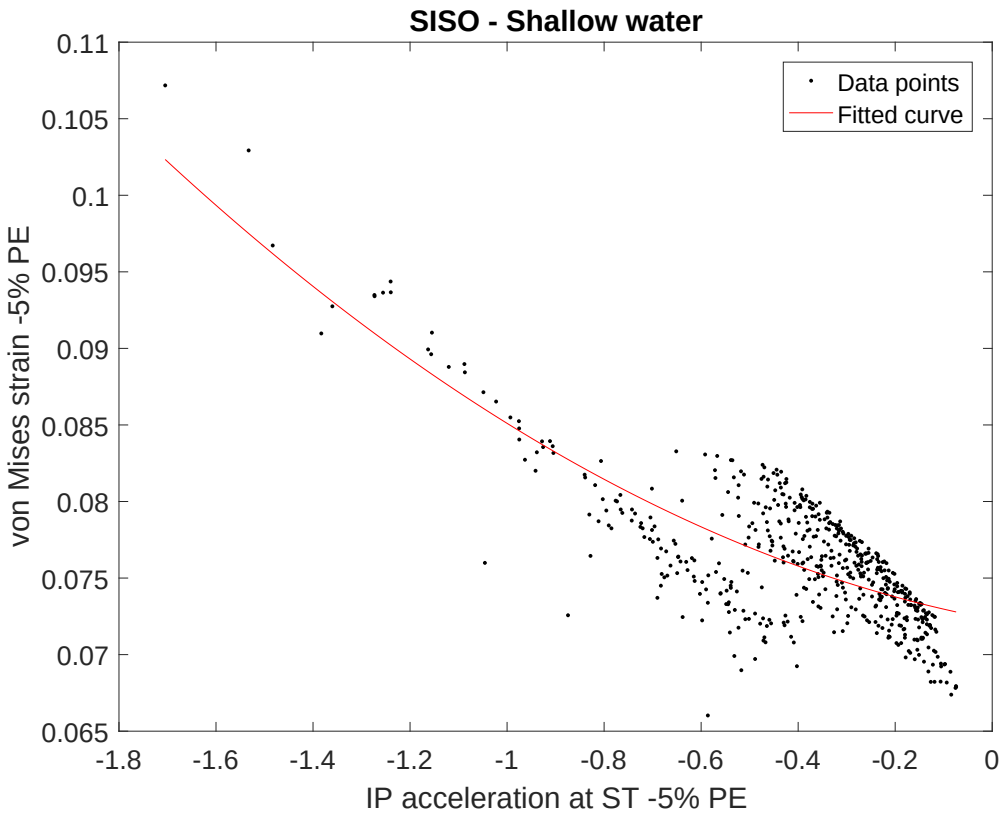

Figure 4.2: SISO - Shallow water

4.3. Multiple-input, Linear regression model (MIR)

4.3.1. Deep water

The in-plane angle θ_{ip}, is based on the *process correlation method* because of the linear relationship between suspended length (TDP) and vessel motions.

Table 4.5 details the results for the deep water case. Figure 4.3 shows the respective error scatter of the output (black dots) along with the model fit to the data (red line).

Table 4.5: MIR results - Deep water

Parameter	Result
θ_{ip}	147 $degrees$
n_o	3
w_o	12 $seconds$
p_o	5%
X_{dom}	In-plane velocity, X_2
Input variables	X_2 - In-plane velocity
	X_{11} - Pitch velocity
	X_{12} - Pitch acceleration
Regression formula	$Y_{pred} = 0.0875 \cdot X_2^{5\%} + -0.0693 \cdot X_{11}^{5\%} + -0.074 \cdot X_{12}^{5\%}$
Error function	$Y_{final} = 1.99 \cdot Y_{pred}^2 + 0.288 \cdot Y_{pred} + 0.05048$
Spread, S	0.0845
RMSE - Error model	0.0097

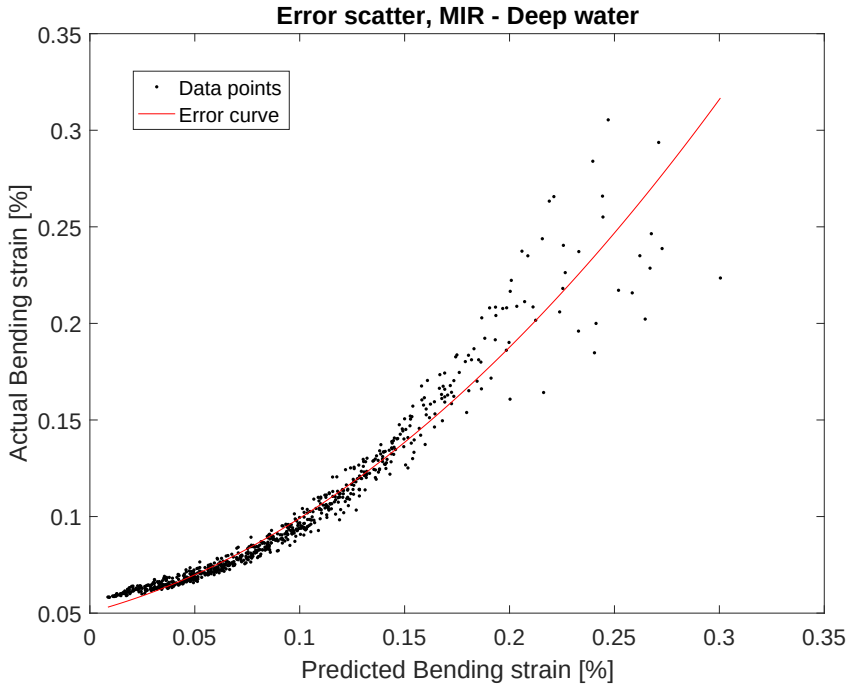

Figure 4.3: MIR error scatter - Deep water

4.3.2. Shallow water

Because of the shallow water depth and stiff pipe, this case has an near horizontal departure angle, low suspended length and high suspended weight of pipe. This causes the small motions of the vessel to cause high tension fluctuations, resulting in a non-liner process. There-

fore, as stated in section 3.7, the *Extreme value correlation method* is used to determine the optimal in-plane angle θ_{ip}.

Table 4.6 details the results for the shallow water case. Figure 4.4 shows the respective error scatter of the output (black dots) along with the model fit to the data (red line).

Table 4.6: MIR results - Shallow water

Parameter	Result
θ_{ip}	162 $degrees$
n_o	3
w_o	4 $seconds$
p_o	10%
X_{dom}	In-plane acceleration, X_3
Input variables	X_4 - Out-plane motion
	X_3 - In-plane acceleration
	X_7 - Roll motion
Regression formula	$Y_{pred} = -0.006 \cdot X_4^{10\%} + -0.0902 \cdot X_3^{10\%} + 0.0088 \cdot X_7^{10\%}$
Error function	$Y_{final} = 1.326 \cdot Y_{pred}^2 + 0.1248 \cdot Y_{pred} + 0.07568$
Spread, S	0.0554
RMSE - Error model	0.0048

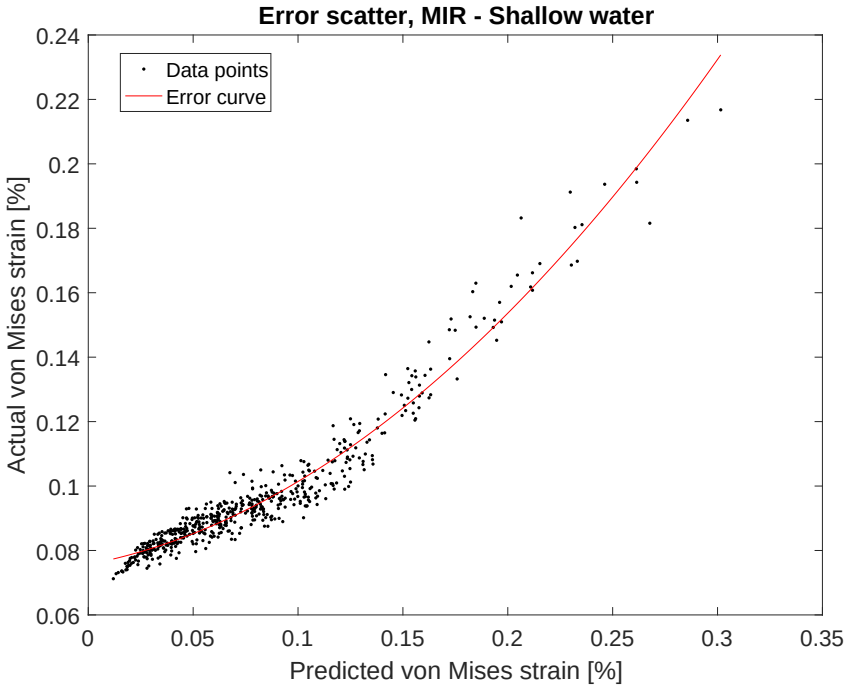

Figure 4.4: MIR error scatter - Shallow water

4.4. Multiple input, Piece-wise linear, Regression model (MIPR)

The MIPR method consists of two datasets for each case. The split of data is based on the *dominating* variable as explained in 3.8. *Dataset 1* represents the lower part of the motions and output strains whereas *dataset 2* represents the higher motion ranges along with its respective strain outputs.

4.4.1. Deep water

Table 4.7 shows the output of the MIPR method along with the respective formulas. Figure 4.5 shows the error scatter of the MIPR method along with the fitted model.

Table 4.7: MIPR results - Deep water

Parameter	Result
θ_{ip}	147 $degrees$
n_o	3
w_o	12 $seconds$
p_o	5%
X_{dom}	In-plane velocity, X_2
Dataset 1	
Input variables	$X1_1$ - In-plane motion
	$X1_2$ - In-plane velocity
	$X1_{11}$ - Pitch velocity
Regression formula	$Y1_{pred} = 0.0004 \cdot X1_1^{5\%} + 0.0273 \cdot X1_2^{5\%} + -0.0248 \cdot X1_{11}^{5\%}$
Error function	$Y1_{final} = 21.73 \cdot Y1_{pred}^2 + -2.046 \cdot Y1_{pred} + 0.1057$
Spread, $S1$	0.0219
RMSE - Error model	0.0014
Dataset 2	
Input variables	$X2_2$ - In-plane velocity
	$X2_{11}$ - Pitch velocity
	$X2_{12}$ - Pitch acceleration
Regression formula	$Y2_{pred} = 0.0809 \cdot X2_2^{5\%} + -0.0865 \cdot X2_{11}^{5\%} + -0.1065 \cdot X2_{12}^{5\%}$
Error function	$Y2_{final} = 0.6625 \cdot Y2_{pred}^2 + 0.7959 \cdot Y2_{pred} + 0.01414$
Spread, $S2$	0.0808
RMSE - Error model	0.0114

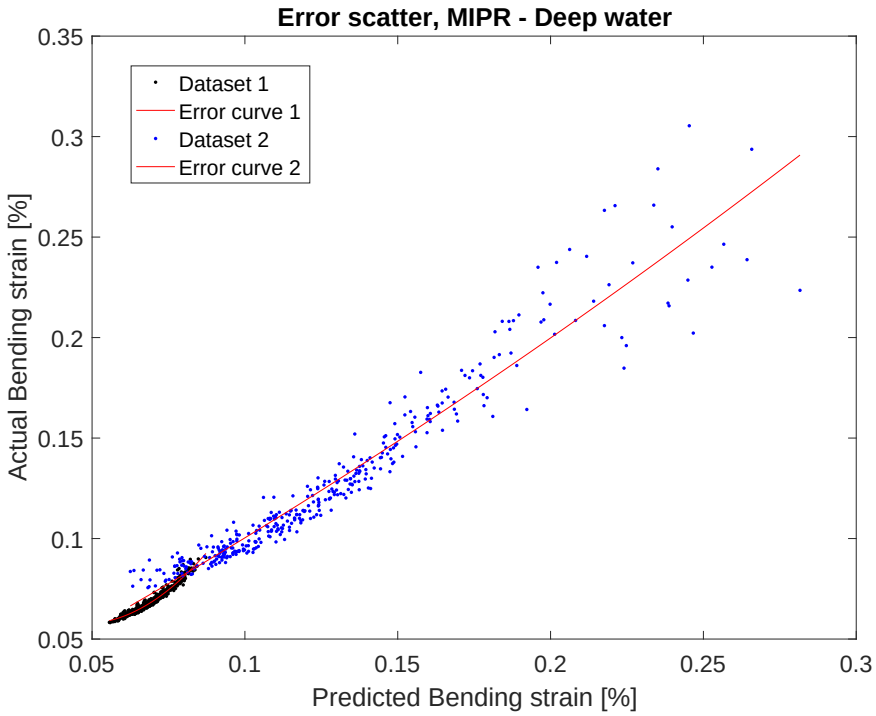

Figure 4.5: MIPR error scatter - Deep water

4.4.2. Shallow water

Table 4.8 shows the results of the MIPR method for shallow water. Figure 4.6 shows the respective error scatter along with the model fit to it.

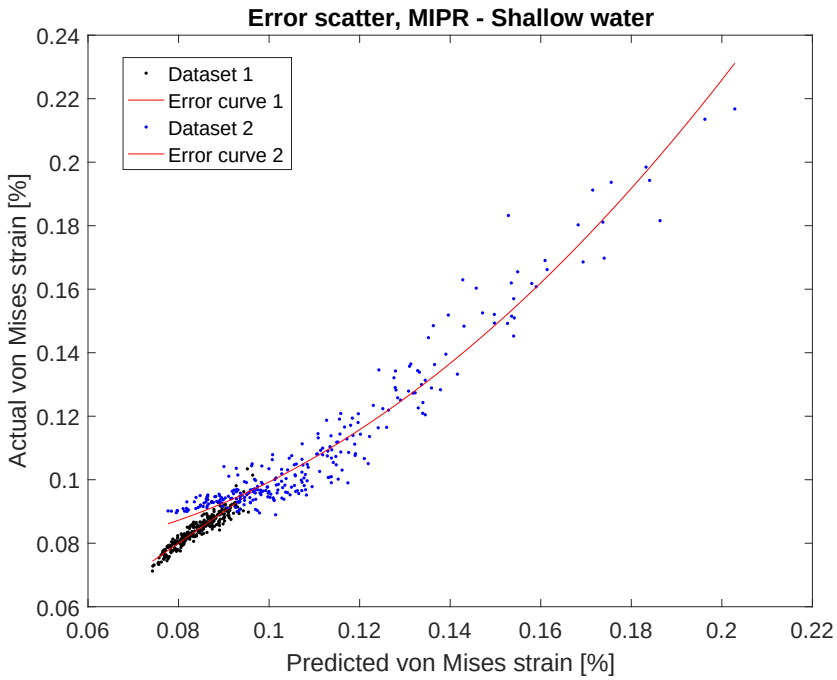

Figure 4.6: MIPR error scatter - Shallow water

Table 4.8: MIPR results - Shallow water

Parameter	Result
θ_{ip}	162 $degrees$
n_o	3
w_o	8 $seconds$
p_o	5%
X_{dom}	In-plane acceleration, X_3
Dataset 1	
Input variables	$X1_1$ - In-plane position
	$X1_3$ - In-plane acceleration
	$X1_{11}$ - Pitch velocity
Regression formula	$Y1_{pred} = 0.0011 \cdot X1_1^{5\%} + -0.017 \cdot X1_3^{5\%} + 0.0182 \cdot X1_{11}^{5\%}$
Error function	$Y1_{final} = 0.992 \cdot Y1_{pred} + 0.0006807$
Spread, $S1$	0.0206
RMSE - Error model	0.0018
Dataset 2	
Input variables	$X2_1$ - In-plane position
	$X2_4$ - Out-plane position
	$X2_3$ - In-plane acceleration
Regression formula	$Y2_{pred} = 0.0008 \cdot X2_1^{5\%} + -0.0026 \cdot X2_4^{5\%} + -0.04388 \cdot X2_3^{5\%}$
Error function	$Y2_{final} = 5.535 \cdot Y2_{pred}^2 + -0.3942 \cdot Y2_{pred} + 0.08337$
Spread, $S2$	0.0561
RMSE - Error model	0.006

4.5. Validation

Now that all the prediction models are complete and the formulas are available, this section validates them for various different sea-states.

4.5.1. General procedure

The following points briefly describe the procedure of validation:

- Firstly, three different sea-states are chosen for each installation case, assuming that these will represent the real time offshore environment.

- These sea-states *do not* belong to the database which was used to create the models of this thesis study.
- The sea-states are of three types:
  1. Uni-directional JONSWAP spectra with direction between 90-180 degrees.
  2. Jonswap spectrum with wave spreading (multi-directional).
  3. Torsethaugen spectra with wave spreading (multi-directional).
- The 15 sets of motions (section 3.5) at the stinger tip[1] of the vessel is recorded, while the vessel response is simulated in the given wave environment. This is done through Orcaflex software. These 15 input time series are the inputs for the model developed in this thesis study.
- From the vessel motion time series, the required input components for each method are extracted and subsequently applied to each model formulae. These input values and their corresponding formula are detailed in section 3.9.
- Once the output strain predictions from the three models are available, they are compared against the actual strain values that result from the time-domain, finite element, pipelay model. In this case, the sea-states are given as input to the Orcaflex pipelay model and the resulting strain output parameters are recorded.
- The error in the predictions of these models are quantified.

Although JONSWAP spectra was used for generating the database, the spectrum direction for validation is chosen between 90-180 degrees, as these directions were not a part of the database generated previously. The Torsethaugen spectra is a typical representation of a spectra with influence of two peaks, one due to swell sea and other due to wind sea. This spectral shape is representative of North-sea conditions.

4.5.2. Input parameters

Table 4.9: Input wave spectra for validation

Case number	Spectrum type	Directionality	H_s $[meter]$	T_z $[seconds]$	θ, θ_p
Deep Water installation case					
1	JONSWAP	Un-directional	2.5	7	140°
2	JONSWAP	Multi-directional	4	8	70 °
3	Torsethaugen	Multi-directional	4	7	30 °
Shallow Water installation case					
4	JONSWAP	Uni-directional	2.5	7	140 °
5	JONSWAP	Multi-directional	3	8	70 °
6	Torsethaugen	Multi-directional	3	6.5	30°

[1]Last roller support on the stinger of the vessel

4.5.3. Results

Figure 4.7 shows the scatter of the values against the various models. It is to be noted that the graphs on the extreme right of figure have two curves, due to the split of database into two sets. The graphs on the first row represent the three sea-states pertaining to the deep water installation case. The second row of graphs represent the three sea-states pertaining to the shallow water installation case.

The Prediction error and the percentage error used in the tables can be explained by the following equations:

$$Error = Y_{actual} - Y_{pred}$$

$$Percentage\ error = \left(\frac{Y_{actual} - Y_{pred}}{Y_{actual}}\right) \times 100$$

where Y_{actual} is the actual strain output from time-domain simulation and Y_{pred} is the predicted strain output, from one of the three models discussed in this document.

Table 4.10: Validation Results Summary - Deep water case

Deep water case									
Case	**Actual Bending strain**			**Predicted Bending strain**			**Percentage error [%]**		
	SISO	**MIR**	**MIPR**	**SISO**	**MIR**	**MIPR**	**SISO**	**MIR**	**MIPR**
1	0.0605	0.0737		0.0604	0.0713	0.0743	0.2786	3.2074	-0.8284
2	0.0756	0.2120		0.0743	0.2811	0.2699	1.6983	-32.5863	-27.3159
3	0.0685	0.1500		0.0678	0.1444	0.1514	1.0032	3.6813	-0.9611

Table 4.11: Validation Results Summary - Shallow water case

Shallow water case									
Case	**Actual von Mises strain**			**Predicted von Mises strain**			**Percentage error [%]**		
	SISO	**MIR**	**MIPR**	**SISO**	**MIR**	**MIPR**	**SISO**	**MIR**	**MIPR**
4	0.0780	0.0932		0.0755	0.0906	0.0918	3.1665	2.8401	1.5792
5	0.0881	0.1657		0.0868	0.1709	0.1388	1.4376	-3.1514	19.2754
6	0.0742	0.1075		0.0784	0.1157	0.1106	-5.5808	-7.6080	-2.8559

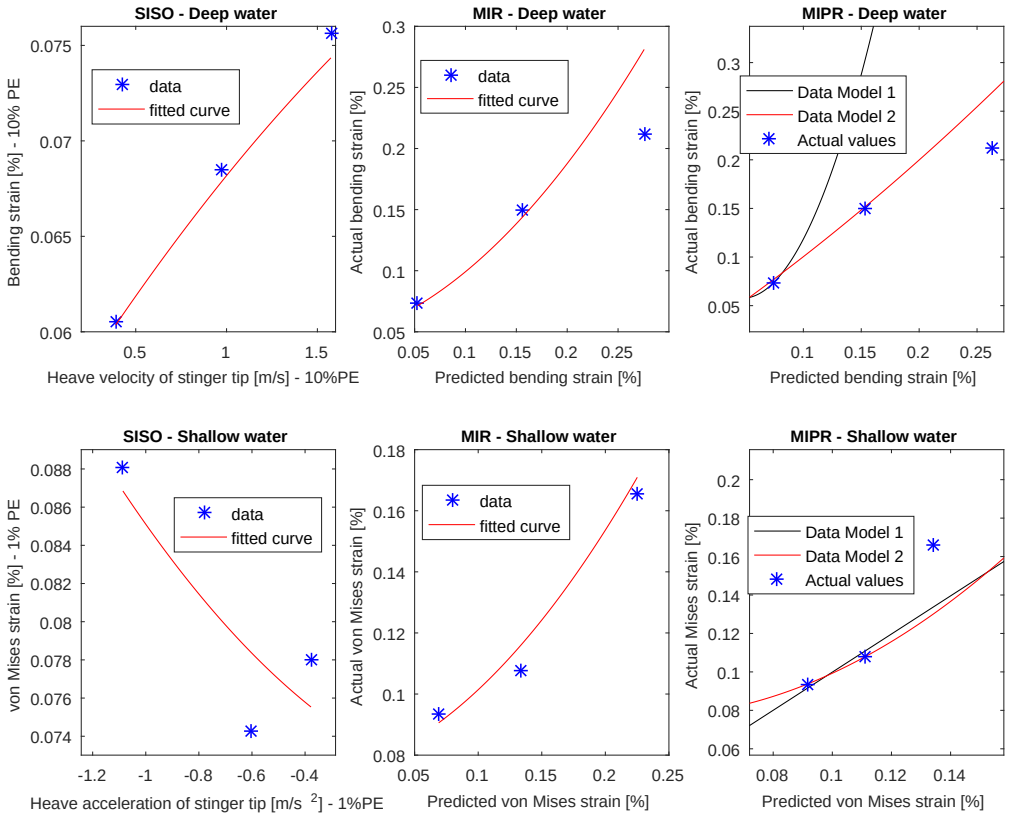

Figure 4.7: Validation Results

5

Analysis & Discussions

This chapter analyses the two installation cases in detail, along with the results of the three methods and their implications. Further, the advantages and limitations of the various methods adopted in this study is elaborated.

5.1. Analysis of results

This section analyses the results presented in the previous chapter.

5.1.1. SISO

The SISO method is the simplest way of representing the output strains with the help of single input variable. Since the spread of the scatter is used to evaluate the relationship between the input and output extrema, any kind of input-output scatter (linear/non-linear) can be analysed in terms of spread.

It can be seen from figure 4.1 and 4.2 that the output of the deep water model shows a better relationship than that of the shallow water case. RMSE values of the fit stated in tables 4.3 and 4.4 also show that the model predictability is better for the deep water case than that of shallow water. This is further proved from the validation results stated in 4.10 and 4.11, where the maximum error percentage of the deep water case predictions are much lower than that of the shallow water case.

The reason why the shallow water pipelay case shows a poor correlation for the SISO method is because of that fact that there is indeed more than one input variable that influences the output maxima and this is not taken into account by the SISO model, causing erroneous predictions. This kind of phenomena is also known as the effect of the *confounding* variable or *third* variable. The deep water case, on the other hand, is physically dominated by the velocity of the pipe in the vertical/near-vertical direction. This is because the near vertical movement of the vessel is in the axial direction of the pipeline, thereby transferring any vertical movement directly to sagbend region, which is at a water depth of about 2000 meters. Also, the very high correlation in the scatter indicates that it is less likely for another variable to have a comparable effect on the output strains.

Another interesting thing to note in the output graph of the shallow water case (5.3) is that the data shows two separate regions, each with a unique trend in scatter. The corresponding strain regions overlap each other to a certain extent. Data group 1, lies in the low strain region and

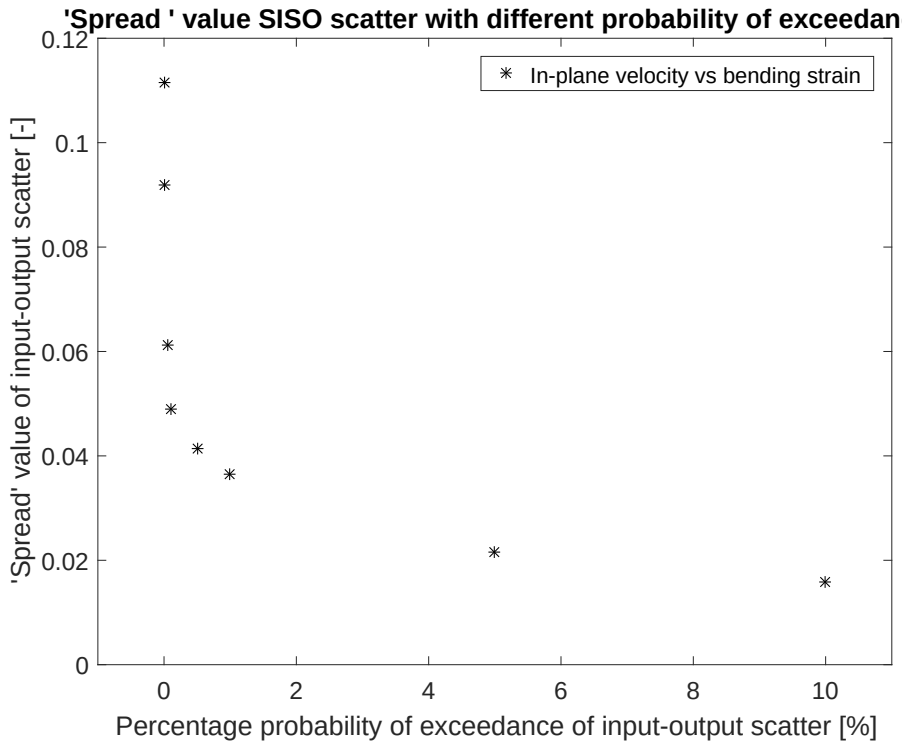

Figure 5.1: Spread of SISO values corresponding to different probability of exceedance (Deep water installation)

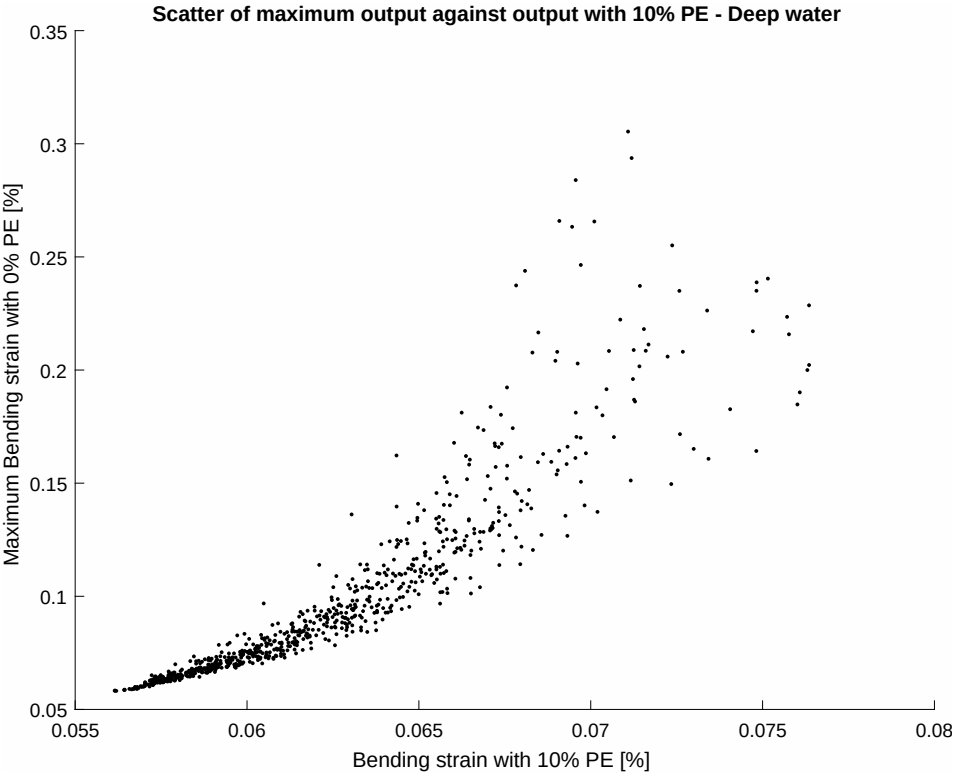

Figure 5.2: Scatter of bending strain output with 10% probability of exceedance against maximum bending strain (Deep water installation case)

shows considerable amount of dispersion in its scatter. The data in group 1 also corresponds to low input motion amplitudes. The range of group 2 however is very large (extends over a large portion of the strain range as well as the input motion range), but the dispersion is relatively low when compared to that of group 1. The current output of the SISO model fits a common curve through both these groups of data, which decreases the overall reliability of the model. Identifying these separate data groups and subsequently fitting a line or curve through them separately will lead to much better predictions of the output.

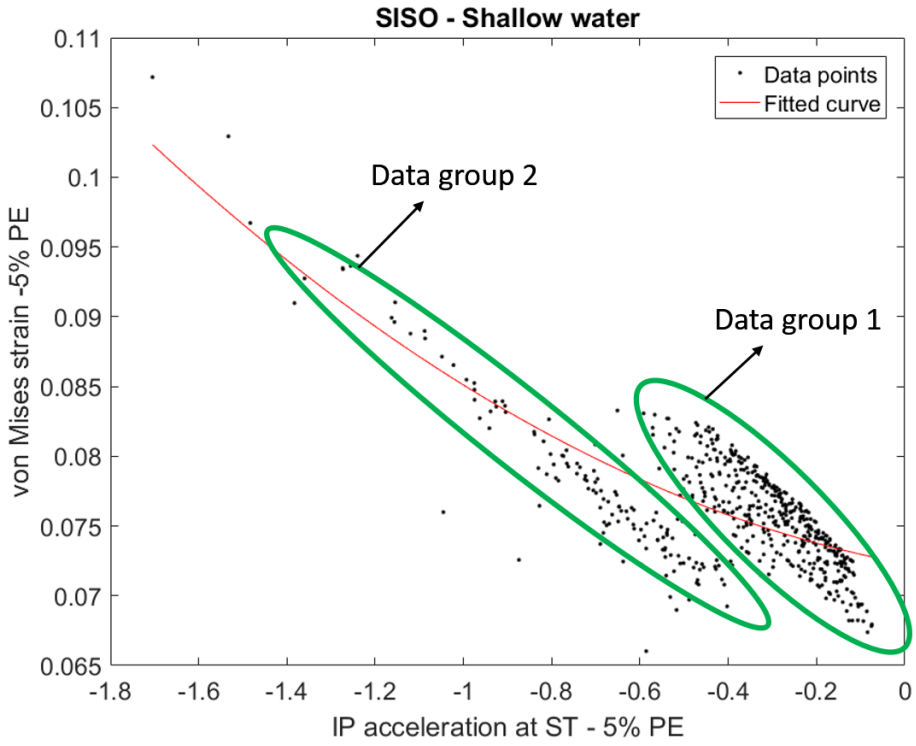

Figure 5.3: Analysis of SISO scatter in shallow water showing two distinct patterns

In conclusion, The SISO method is a good way to predict the maxima of the output variable, given that there is no other variable affecting the relationship between input and the output variable. A disadvantage of the SISO method is that although it gives good predictions of the output maxima corresponding to a certain probability of exceedance, the predictions are unreliable for the input-output scatter with a probability of exceedance of 0% (absolute maxima/extrema). This can be seen in figure 5.1 (deep water case) where the spread of the input-output scatter exponentially increases as we move to the extremes. The reason for this poor correlation is because the occurrence of the maximum output values is chaotic. This can be corroborated by figure 5.2, which shows a poor correlation in the scatter of maximum strain values against the strain values corresponding to 10% probability of exceedance (10% probability is the output of the SISO method in deep water).

The maximum strain output is of importance to the study because of the fact that the maximum strain values should never exceed the given design value during dynamics, in order to ensure integrity of the pipeline. Therefore due to this uncertainty of maximum output values, the SISO model is not preferable.

5.1.2. MIR

The MIR method uses multiple inputs to describe the output maxima, using multiple linear regression and subsequent error correction. The input variable representing the SISO model is taken as the dominating variable for the MIR method.

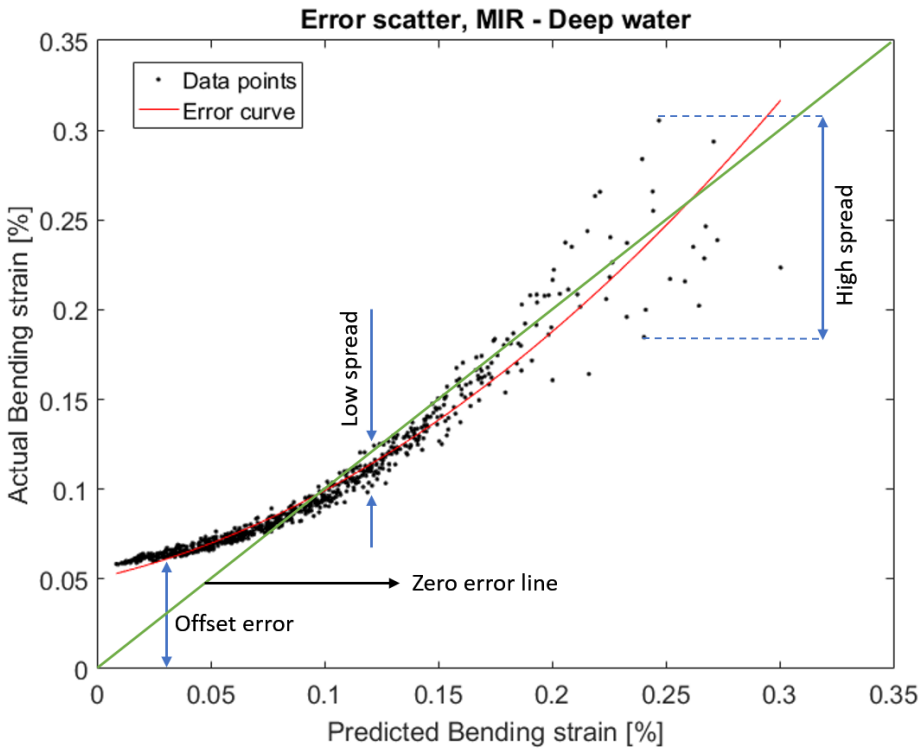

Figure 5.4: Graphical explanation of the error scatter resulting from the MIR method in *deep* water

Deep water This following paragraphs will analyse the deep water installation case in detail. Similar conclusions can be extrapolated for the shallow water installation case. Figure 5.4 reproduces figure 4.3 of the previous chapter, which shows the error scatter of the MIR method in deep water. It can be noticed that the spread of the scatter around the fitted line is less in the low strain region and increases in the region of high strains. This can be explained by the fact that low strains are caused by low motions amplitudes, where the pipelay system almost behaves linearly. Thus, linear regression performed in this region will result in a low error scatter. As the motion amplitudes get higher, the non-linearity of the process increases and therefore when linear regression weights are fit to data, it results in larger spread of the error scatter. This large scatter is because the physical nature of the system in this high strain region is different, either because the regression inputs combine non-linearly, or because there is some other factor that is involved in the process (another influencing variable) that has not been taken into account by the model (during high motions of the vessels, the contributions of non-critical variables such as out-plane motions will increase as any extreme movement in any direction, is likely to affect the suspended length of pipe and its configuration). There is a possibility for both of the above mentioned factors to be present simultaneously. This process of unequal variation of the actual strain output, over the range of the predicted values is known as heteroskedasticity.

Now that the dispersion of data is analysed, it is important to also analyse the gradient of the

error scatter, since this also carries some information about the data. The line running through the graph at a 45^o angle is the zero error line between the predicted and actual scatter. It can be noticed that in the low strain regions, the regression output (predicted output values) underestimate the actual output, since the data points lie above the zero error line. Also, the gradient of the scatter is fairly constant, with a very low dispersion. The gradient of the error scatter is almost on the zero error line, showing that the chosen variable for regression are fairly representative of the process in the medium-high strain region. There are two possibilities for the underestimation in the low strain region, both of which are partially related to each other.

The first possible reason is the problem of *overfitting* in this low strain region. The low strain region could have been sufficiently represented by just one or two motion variables, but the gradient of the third variable sets the predictions off from the actual value. However, the dispersion still remains low despite this extra variable. This is possibly due to a *high partial correlation* between the input motions, at low motion ranges. Partial correlation in terms of this thesis study, is the correlation/interdependence between two inputs X and Y, which also show a correlation with the output. For example, if a maximum In-plane velocity is the driving factor for the maximum strain output at low amplitudes, there might be a possibility that maximum out-plane acceleration, which does not cause the maximum strain might also have a good correlation with the maximum strain, merely because of the fact the In-plane velocity and out-plane acceleration are partially correlated with each other. The second possible reason is that the inputs that are chosen for the entire database are not the optimal choice for this particular low amplitude-low strain region. The underestimation might be due to this reason. Again, the resulting dispersion is still low because of the possibility of partial correlation between variables, as described above. Either way, this does not affect the results, merely because of the fact that this error gradient can be corrected, owing to the low error dispersion in this region. The partial correlation between variable should be further investigated, in order to obtain a better understanding of the process.

The validation outputs presented in table 4.10 prove the conclusions of the deep water case, where the strain value corresponding to the high strain range shows large errors in predictions (case2). The prediction of the strains in the low and medium strain ranges are good (case 1 and 3).

Shallow water Figure 5.5 reproduces figure 4.4, displaying the error scatter of the MIR method in shallow water. The first thing to be noticed is that the dispersion of values is fairly low for the shallow water case, throughout its entire range of values. This indicates that the shallow water case behaves almost *consistently* throughout the database, regardless of whether the behaviour is linear/non-linear. One of the reasons for this is because the shallow water case is only simulated up-to a 3 meter H_s. This is because the system non-linearities are in general higher than the deep water case and therefore increasing the sea-state beyond 3 meters causes the strains to increase un-proportionally, deteriorating the quality of the data on the whole (not desired). Also, the likelihood of pipe buckling occurs at lower strains than that of deep water, because of the added effect of high tension fluctuations in pipeline. Therefore simulating up-to a 3 meter sea state is considered to account for all the strain ranges of interest, with respect to the integrity of pipeline. Therefore, it can be concluded that due to this low dispersion in values, the variables assumed for regression are representative of the process throughout the database.

The second thing to be noticed is that the gradient of the error does not lie on the zero-error line. Also, this gradient is fairly constant with a positive slope. The error due regression pro-

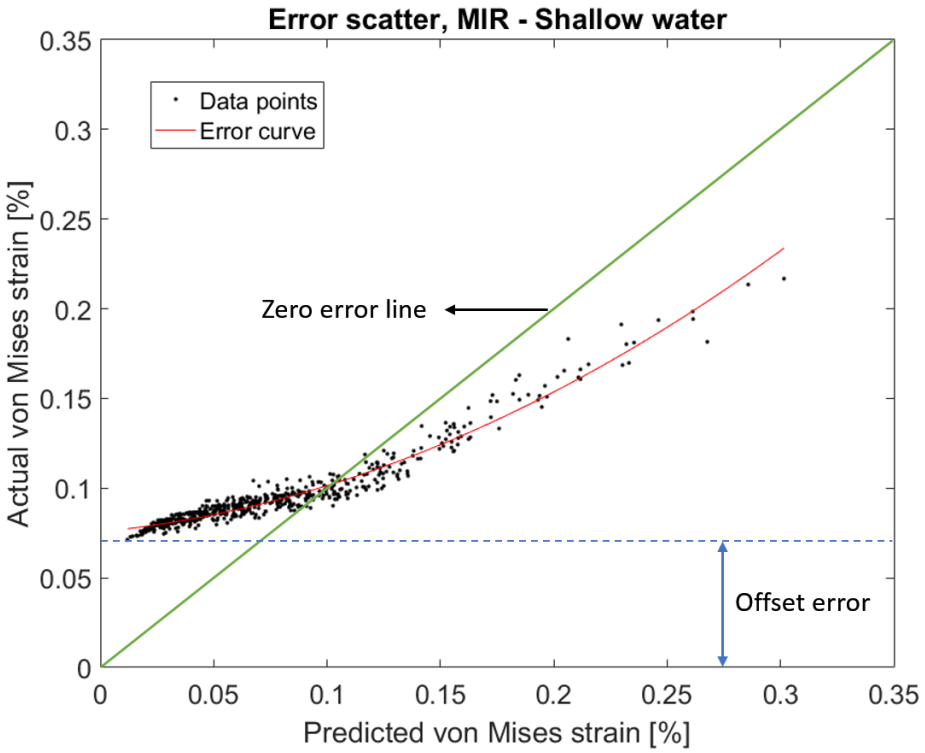

Figure 5.5: Graphical explanation of the error scatter resulting from the MIR method in *shallow* water

gressively reduces, from the region of underestimation (for low strain ranges) to the region of overestimation (high strain ranges). The reason for this is that the regression coefficients are not optimal for the entire database. The reason for the low spread is because of the consistency of the database as described in the previous paragraph (also due to optimally chosen input variables). Splitting the database should help overcome this constant error gradient and place the values along the zero error line. Section 5.1.3 proves this statement.

In conclusion the shallow water prediction model is more reliable than the deep water case. This is corroborated by the validation results stated in table 4.10 and 4.11, except for the Torsethaugen spectra in case 6, which shows a error of -7.6%. The percentage error of MIR predictions is low for the first two cases, especially for the high strain region (case 5 better than case 2).

5.1.3. MIPR

The aim of the MIPR method is to overcome the issue stated in the previous section, regarding the grouping of datasets with different behaviour in the same pool, leading to non-optimal results. The MIPR method aims to split the database into groups of similar behaviour, such that subsequent regression on these split datasets will lead to a more consistent error pattern which can be corrected to obtain better predictions of the output maxima.

The figure shows that the MIPR output for both cases shows an error gradient that almost lies on the zero error line, proving that the split of database overcomes the non-optimal regression coefficients that were fit for the entire database. Splitting the database resulted in grouping of data with similar behaviour, thereby reducing error due to regression coefficients.

Another important point to note is that splitting the database now results in a lower spread

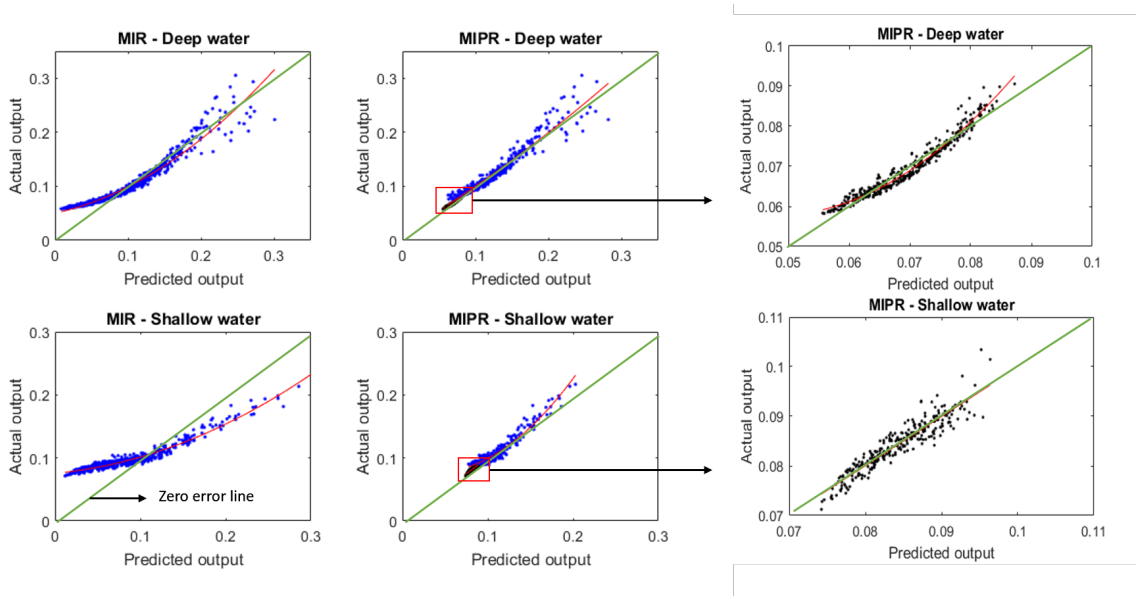

Figure 5.6: MIR and MIPR model comparison

(dispersion) of values in both the datasets. This is because the variable combination chosen for regression, are now different for each database, as they have been chosen separately for an optimal combination. The first dataset, represented by the two graphs on the extreme right of the figure have a minimal error correction function, with a high predictability (low dispersion). It should be said that even though the spread of values in high strain region has decreased for the deep water (when compared to MIR method in deep water), the spread is still significant, thereby decreasing the reliability of MIPR method high strain regions. The reason for the high spread even after splitting the database is because, the regression method assigns linear weights to a process that is inherently non-linear.

Tables 4.10 and 4.11 show the validation results of the two installation cases. The improvement of results is clearly visible in deep water, where the percentage error has been reduced significantly (especially case 2). This is also the case for shallow water except for case 5 (Torsethaugen spectra with a 4 meter H_s), which shows an underestimation by the MIPR model of about 20%. This is in the high strain region of the graph shown in figure 4.6. The major reason for this error is due to the lack of sufficient data points in this region. More data might result in a better model fit for the error scatter, thereby increasing the reliability of predictions.

5.2. Discussions

5.2.1. Pipelay system behaviour

It is known that the pipelay is non-linear and thereby solved in the time-domain. However, it is useful to know the extent of this non-linearity, for a given installation case. This can be done with the help of correlation coefficients. It should be noted that correlation coefficient can only be used to identify the linearity of the process. Each database simulated in this study consists of R simulations, which range from small to high sea-states. The database therefore contains regions of linear and non-linear behaviour of the system. The distribution of these coefficient values will provide an insight to the extent of linearity/non-linearity that exists between the output and any given motion input. Figure 5.7 shows the distribution of

the correlation coefficient of the *vertical velocity of stinger tip* for the shallow and deep water installation case.

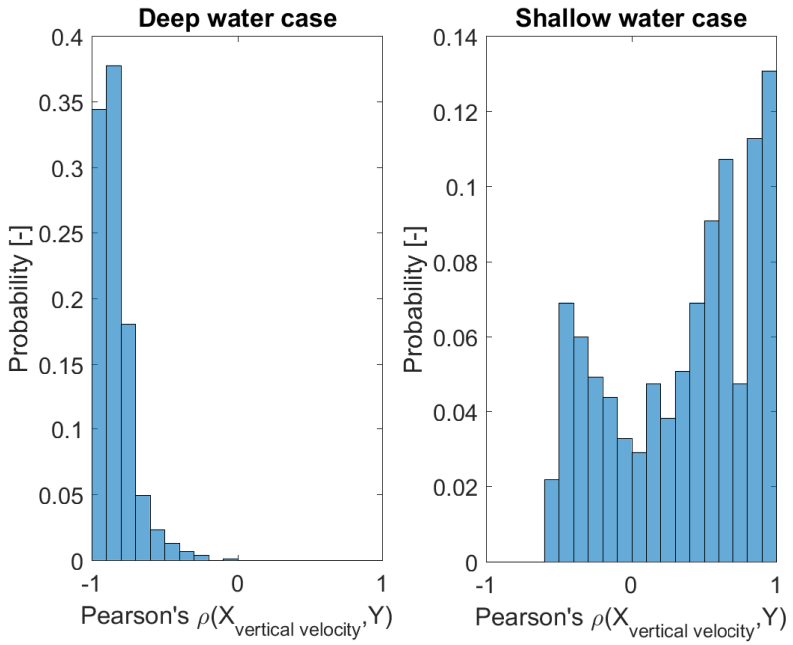

Figure 5.7: Distribution of Pearson's correlation coefficient - Vertical ST velocity and Output strain

It can be seen from the figure that about 75% of the simulations in the *deep water* case show a high correlation magnitude above 0.8, indicating a *strong* linear relationship between the given input variable and output. The few simulations that show bad correlation are more likely to have a high sea-state input and therefore high vertical velocities. Such a system with high vessel motion ranges behaves non-linearly, thereby introducing an uncertainty in the physical process in that region. Thus it can be said that the deep water pipelay case is linear over a large range of the database. In contrast to the deep water case, the vertical velocity in shallow water is widely distributed with a high variance. The peak corresponding to the highest ρ magnitude corresponds to only 25% ($\rho > 0.8$) of the entire database, which is a relatively low percentage of the entire population. The ρ values for the remainder of the simulations are widely scattered, indicating an uncertainty of the nature of the physical process. Therefore, the non-linearities of the shallow water system come into play, at much lower sea-states (lower motion ranges) when compared to that of deep water. This is because of the high sensitivity of the TDP variation with respect to vessel motions (high tension and near-horizontal pipe departure).

The following conclusions can be drawn from the above discussion:

1. The dispersion of correlation coefficients between the input and output gives an idea of the homogeneity of system behaviour throughout the database.
2. Given a low variance/standard deviation of the corresponding distribution, the average value of correlation coefficient quantifies the amount (strength) of linearity of the physical process.

For a given input-output ρ distribution, the average value of Pearson's correlation determines the amount of linear influence that an input variable has on the output. However, this method

of quantifying the input-output relationship is limited by the fact that a low average correlation can either mean that the respective input does not have an influence on the output, or that it has perfectly non-linear relationship which is not recognised by a linear operator such as Pearson's ρ. It is therefore appropriate to use ρ for installation cases that are known to be predominantly linear (low standard deviation) throughout the database.

It should be noted that the overall strength of the relationship, which is given by the mean value of the distribution, is only relevant to the input parameter under study and therefore is not representative of the entire parameter space.

5.2.2. In-plane angle

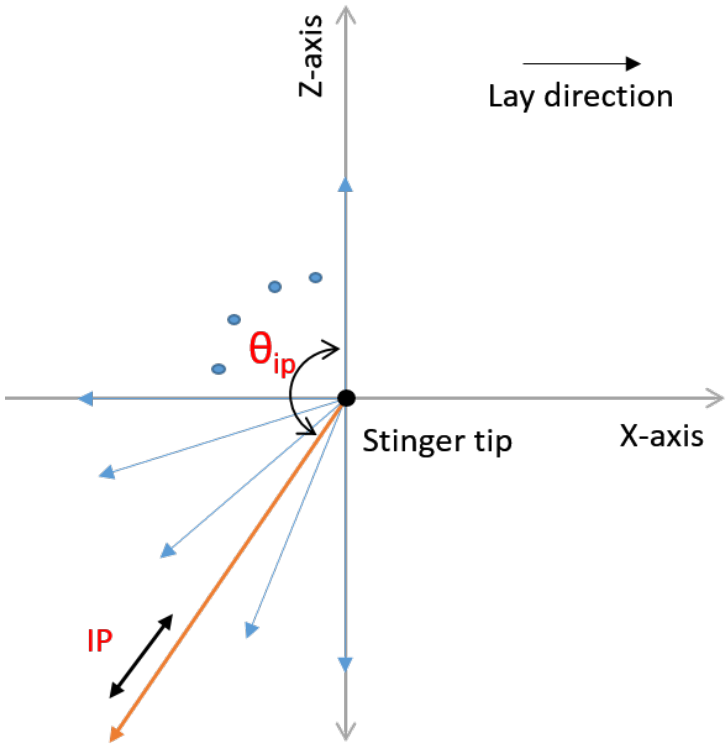

Figure 5.8: In-plane reference direction

As stated in chapter 3, the reference system for pipe motions need not be similar to that of vessel conventions. It is also known that the motions of the vessel about the *stinger tip* is representative of the motions of the top end of the suspended pipeline. Therefore motions about the stinger tip directly control the response of pipeline in the sagbend. It is also known that the motion of the stinger tip in the plane of bending of pipeline has the maximum impact on the pipeline response in the sagbend amongst all other stinger tip motions.

Therefore, the in-plane motions of the stinger tip are referenced about an axis that shows the best correlation with the output variable. The angle of rotation of this in-plane axis from the vertical, is termed as the in-plane angle, θ_{ip} (See figure 5.8).Two methods have been defined in this thesis to obtain the in-plane angle. The choice of these methods depends on the statistical model under consideration.

SISO model

For the SISO model, the *extreme value correlation* method is used, to define the best choice of in-plane angle. The reason for choosing the extreme value correlation is because the SISO model only looks at the extremes of the input and output, and therefore the process details are not of importance. The extreme value correlation method chooses the optimal in-plane angle from a set of angles θ_k, by looking for the angle about which the in-plane motion extrema show the best correlation with the output. Since extremes can refer to various levels corresponding to certain probability of exceedance; the average correlation is taken amongst all the extrema, in order to guarantee that the motions about the chosen in-plane reference will have a good overall correlation with the output maxima. The method of describing correlation between input and output is based on the *spread* of its corresponding scatter. Detailed procedure of SISO method and of calculating the spread of an input-output combination are stated in sections 3.6 and 3.2.3.

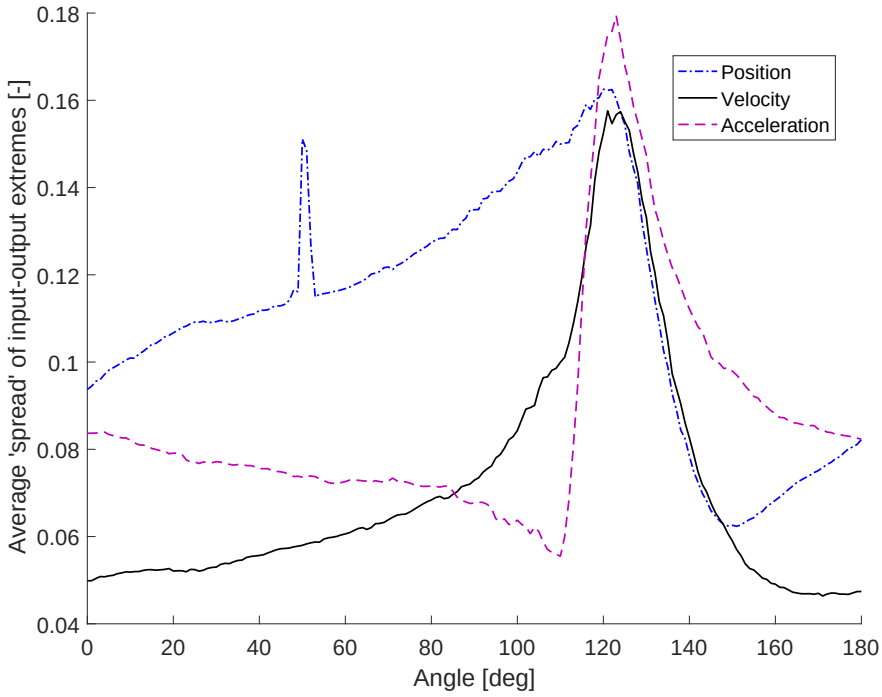

Figure 5.9: θ_{ip} sensitivity - SISO method in deep water

Figures 5.9 and 5.10 show the variation of the average spread values of the input-output extremes with respect to changing angle of in-plane reference, for deep and shallow water cases under consideration. A high value of spread means a high scatter of the input-output values and therefore a poor correlation of the input variable with the output. The vice versa holds for a low spread value. The first thing to be noticed is that the position variable has the least correlation with the output, for both shallow and deep water installation cases. The second thing to be noted is that there exists a region in which all input variables are poorly correlated with the output (peak in graphs). This region is between 100-160 degrees in deep water and 80-110 degrees in shallow water.

For deep water, this area lies in the region between the axial (166^o[1] in the static case) and

[1]The angle of 166^o is with respect to the vertical axis in the upward direction. Same reference as θ_{ip} from figure

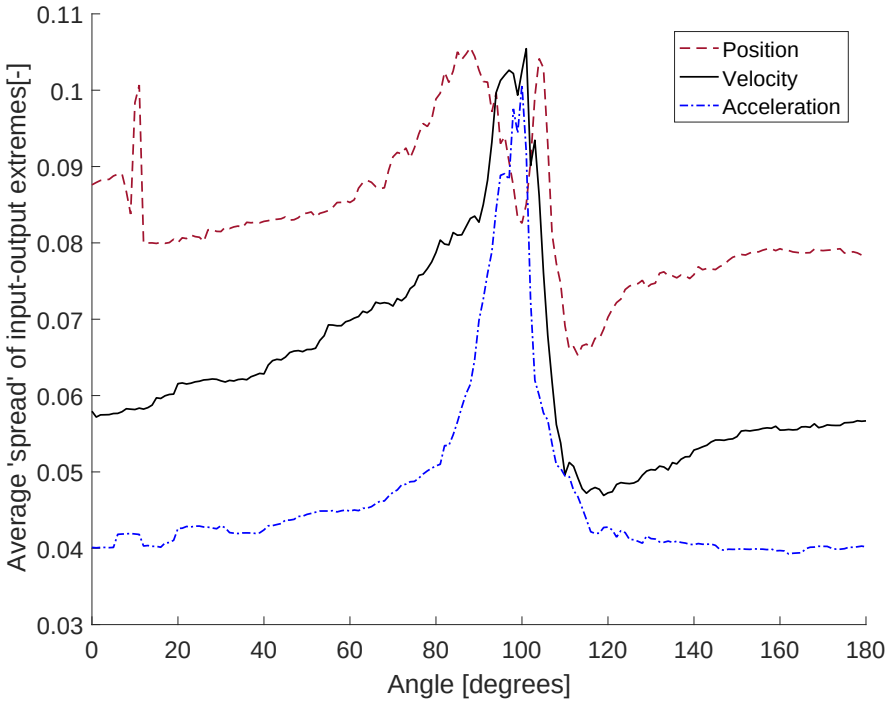

Figure 5.10: θ_{ip} sensitivity - SISO method in shallow water

normal (76^o) direction of the pipeline near the stinger tip. Movement about the axial pipeline direction has a direct effect on the sagbend region which is at a large water depth. Extreme movement about the normal direction will also be transferred to a certain extent in form of bending of the sagbend region of the pipeline. However, any extreme movement about this mid-region cannot cause a maximum bending in the pipeline and therefore the correlation between the extremes is bad in this range of angles.

The reason for the velocity component to show the best correlation for deep water case, is probably because the drag forces acting on the pipeline is proportional to the velocity of pipeline movement and therefore the velocity of the vessel has the best correlation with the output. The optimal angle chosen for the deep water method is 171^o. In the case of shallow water pipelay, the region of poor correlation lies in the surge (horizontal) direction of the vessel. The optimal angle chosen for the shallow water method is 162^o.

Effect of averaging spread values for different extreme levels is explained here. As seen in figure 5.9 and 5.10, there exists a clear region of poor correlation while the remaining regions have a low, constant spread. This is however the average spread of values for different levels of extrema (corresponding to different probability of exceedance). Figure 5.11 shows the spread of the in-plane velocity component in shallow water, over different angles. It can be seen from the figure that the peaks of the velocity variable at different levels of exceedance probability, correspond to the peak from averaging the different extrema(figure 5.10). Instead of averaging, if the in-plane angle was chosen based on the least overall spread among all extreme levels, the result might be a different angle than that obtained by averaging. However, the difference would be negligible because of the constant spread of both the graphs, outside the peak region. This justifies the choice for averaging the correlation (spread) among different

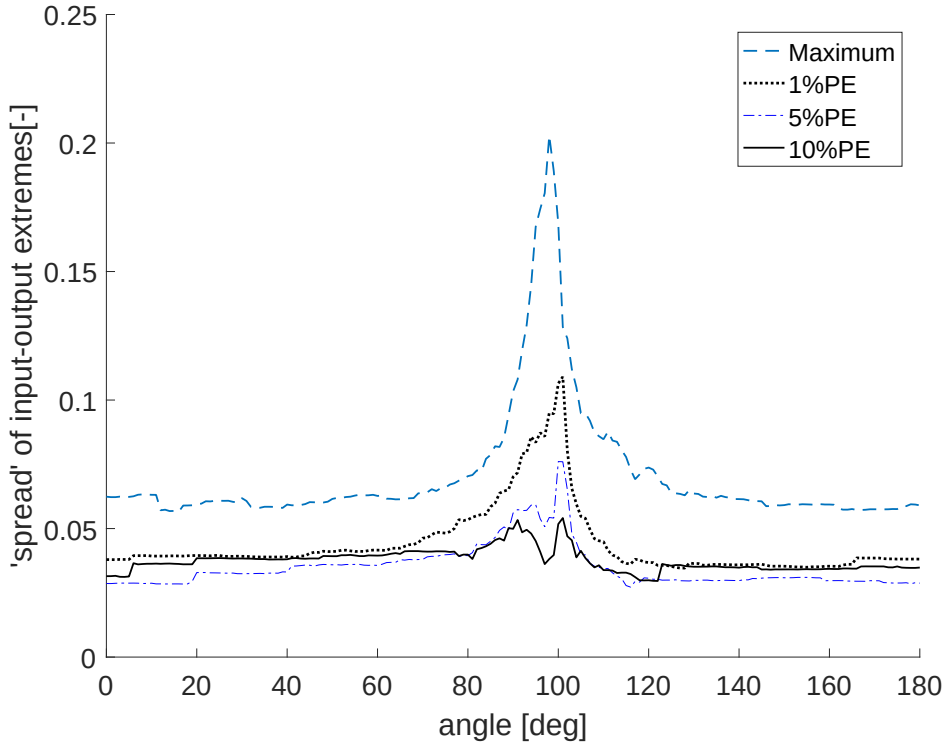

Figure 5.11: θ_{ip} sensitivity for different levels of extrema of the velocity component in shallow water

extrema. Using the averaging method ensures a good overall correlation between the tails of the input and output distribution, thereby ensuring reliable predictions for the MIR and MIPR methods (θ_{ip} based on averaging will lead to better inputs for regression).

Multiple input models (MIR, MIPR)

The choice of θ_{ip} for multiple input models, depends on the system behaviour. In shallow water, the system is known to behave non-linearly and therefore *extreme value correlation* is a good way to find the best angle θ_{ip} based on the extremes, thus avoiding the complexity of the entire process. The extreme value correlation method has been detailed in the previous section.

In deep water however, the system mostly behaves linearly and therefore basing the choice of θ_{ip} on the process gives reliable results. Figure 5.12 shows the variation of the correlation coefficient (ρ), for different angles in the X-Z plane.

It should be noted that a high ρ magnitude means that the strength of correlation is high. The graph of the process correlation method is somewhat similar to that of the extreme value correlation method from the previous section, except that the region of poor correlation is smaller than that of the previous case. This can be explained by the fact that even though the extremes of a simulation show bad correlation with te output, the linear process in between has a very good correlation, thereby causing the high correlation. The optimal in-plane angle for this case is 147^o.

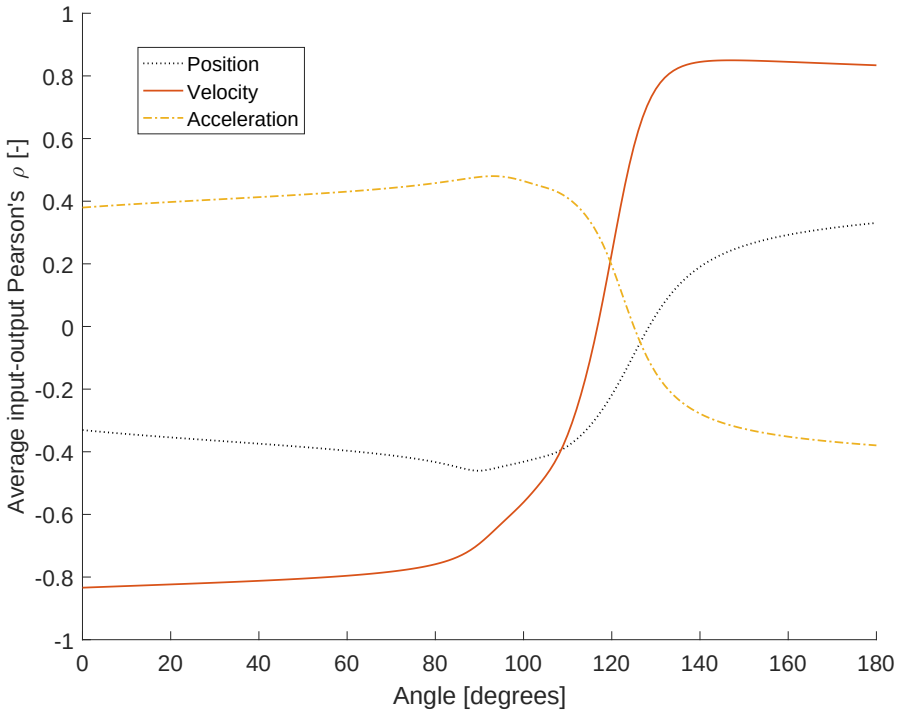

Figure 5.12: θ_{ip} sensitivity - MIR,MIPR method in deep water

5.2.3. Spread function

All the models developed in this thesis study use the *spread function* to choose the best correlation. Therefore it is important to elaborate on the spread function and its implications.

Figure 5.13 reproduces the figure shown in chapter 3. The spread function uses finite windows over the range of the input, whose locations are chosen at definite intervals over the input range. Each window length is chosen such that it is small enough to represent a unique input value and large enough to accommodate sufficient number of data points in the window, for its statistical relevance. The advantage of basing such windows on the input range is that, this makes the process of choosing windows consistent and insensitive to the input variable.

Also, the windows are only located up to 75% of the range of the input,X. This is because it is more likely that the quantity and quality of data points beyond this range is poor. Poor quality means that the data above 75% of the input range will lie in the high strain region, and is likely to have a high spread that will deteriorate the overall spread output. In such a case, the method would not be very robust in choosing the best input-output combination. The implication of choosing finite windows over the range of data points is that the function does not work with 100% of the data. However, this can be advantageous in terms of filtering the unnecessary regions of the scatter.

Within each window, the *coefficient of variation* (c_v) of the scatter is evaluated. This c_v value is then averaged over all the windows, to obtain the spread of the scatter. Although this average value if useful to quantify the *overall* spread of the data combination, it is useful to know how the c_v values are dispersed in a certain data combination. The variance/standard deviation of the c_v values can give information on the amount of heteroskedasticity (increasing spread of values at higher ranges) present in the given combination. For example, this measure of

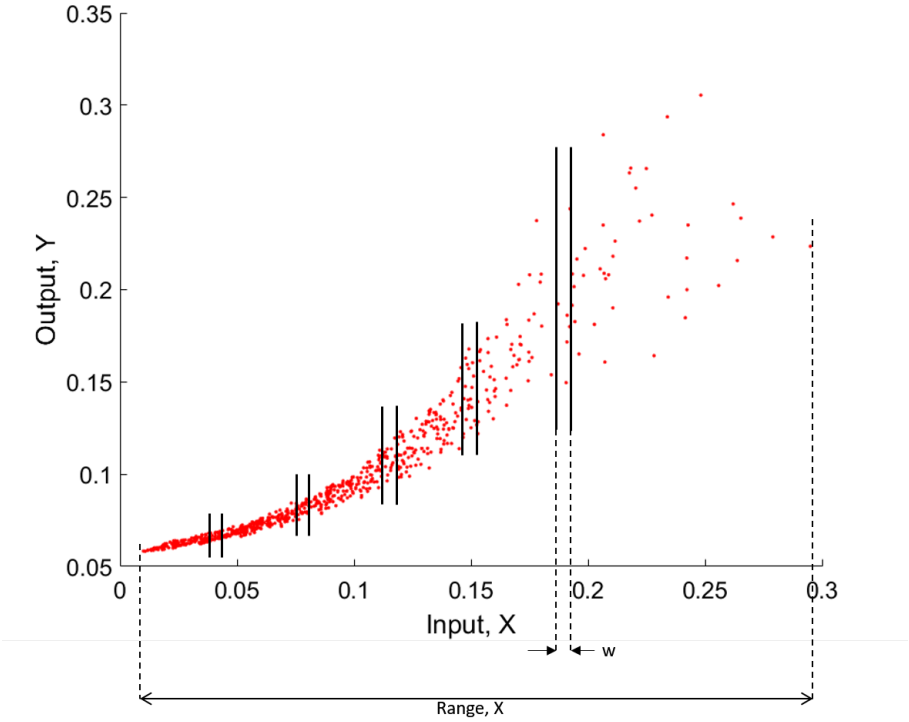

Figure 5.13: Method of determining scatter spread

dispersion in c_v, could help in understanding the heterogeneity of the physical relationship between the given input and output variable.

The spread function can also be improved to concentrate on the areas of interest in a given scatter by giving appropriate weights to respective windows. This for example, will help in identifying error scatter that show least spread of values in particular areas of interest.

Therefore, the spread function is a useful way of quantifying the dispersion of the scatter, in terms of the coefficient of variation, which is a unit-less quantity. The method is robust in filtering different kinds of input-output combinations.

5.2.4. Effect of linearisation on output predictability

The pipelay system is a non-linear process that is solved in the time domain. The non-linearities include the non-linear stress-strain relationship of the pipeline material (only relevant for the overbend part of the catenary, which is not of interest to the problem), non-linear drag loads on pipeline, geometric non-linearity of the suspended catenary, non-linear tension compensation, etc. Most of these parameters can be linearised except for the geometric non-linearity of the catenary. This is due to the presence of *bending stiffness* in the pipeline. As discussed in section 2.2, the catenary can be modelled as a non-linear beam with large deflections, in order to obtain accurate solutions for any installation case. Exact analytical solutions can be obtained if the bending stiffness of the pipeline is neglected (natural catenary method); but this would lead to erroneous results.

If all the other aspects of the system were linearised except for the method of solving the catenary, then the system linearity would depend of the installation case under consideration. A deep water system, where the pipe leaves the vessel vertically, would behave in a fairly linear

manner, considering the major non-linearity which is the drag loads on the pipeline, have been linearised. The tension fluctuations are mostly linear for the deep water case, unless the vessel motions are very high. Therefore the model predictions of all the three models (SISO, MIR and MIPR) would give much better predictions because of low scatter spread. This is because the homogeneity of the system would be prevalent over the entire range of the database. The SISO method in deep water currently predicts output strains with a 10% probability of exceedance. Linearising the system will enable the method to predict even higher levels of strains, corresponding to a probability of exceedance of less than 10%. The multiple input models (MIR, MIPR) would have a constant error gradient because of the homogeneity of the system that would result in the choice of linear regression inputs to be representative of the entire database. The spread of the scatter would also decrease, thereby increasing model reliability. The scatter spread would still increase at very high motion amplitudes because of the high (non-linear) tension fluctuations.

For the shallow water case however, the system would still be non-linear because of the non-linear tension fluctuation due to vessel motions. Although this is also the case for deep water, the non-linear tension fluctuations in deep water only occur at high motions amplitudes, unlike the shallow water case, where this non-linearity is prevalent even for small motion amplitudes. The major reason for this is the small suspended length of pipeline, coupled with the high set tension and near horizontal departure angle. No solid conclusion can be made about the SISO method, as it is more likely that there is still the presence of the other (confounding) variable which also influences the output strains, that has not been taken into account by the model. This is already seen in the fully non-linear case for shallow water considered in this thesis study, where the input-output correlation is bad (validation outputs also bad due to the effect of the confounding variable (5.1.1)). The error scatter of the multiple-input models is likely to show a constant gradient. The spread of the error scatter is likely to improve (less dispersion), although it may not be to a considerable extent. The linear tensioner model in the shallow water case would ineffectively compensate non-linear tension fluctuations and therefore high strains are expected. This is not the case in deep water, since the tension fluctuations are usually low.

Thus, possible linearisation of the pipelay system is expected to make all three models more reliable in the case of deep water. For shallow water however, the SISO method is not expected to show much improvement due to the presence of the confounding variable. The multiple input models will improve, but the degree of improvement is not expected to be as high as that of the deep water case.

6

Conclusions & Recommendations

6.1. Conclusions

The main focus of this thesis study is to find a relation between vessel motions and pipeline integrity in the sagbend region of the catenary. This is done with the help of *three* statistical models that were developed during the course of the study, namely:

1. Single input - Single output model.
2. Multiple input, Linear Regression model.
3. Multiple input, Piecewise-linear, Regression model.

All these models require the generation of a database of pipeline models during project preparation, after which post processing is carried out on the database, in order to arrive at formulas that employ a quick interpolation method to predict the extreme pipe response. These formulas can be used against any vessel motion input, to quickly determine the maximum strains likely to be experienced, for the anticipated sea state offshore.

Since the motions of the vessel and top tension in the pipeline are closely related, and since tension is the governing parameter for pipeline response, the current tensioner model used by Allseas was improved by accounting for the velocity limitation of the tensioners. The model was subsequently used for further analysis.

The above listed statistical models were developed for two different installation cases, one is a deep water case in a water depth of 1500 meters and a relatively flexible pipeline of 20 inch outer diameter. The other case is in a shallow water depth of 122 meters, with a very stiff pipeline of 44 inch outer diameter. The models developed for both these installation cases are validated for a total of 6 dynamical sea-state inputs, which are *not* a part of the initial database.

The velocity of the vessel about the axis referenced along the plane of bending of pipeline (in-plane velocity), is the variable chosen to represent the SISO system for the deep water installation case. This variable is considered to have the most dominating influence on the output maxima (*dominating* variable). The corresponding variable for the shallow water case is the acceleration of the vessel about the same in-plane axis (in-plane acceleration). The SISO system for the given installation cases, results in a relation between input and output values corresponding to a certain probability of exceedance. The model is however unreliable in predicting the maximum output values, as shown in section 5.1.1 and figure 5.1.

The MIR model gives reliable predictions for the shallow water case. In the deep water case, the reliability of the model reduces for high strain regions. The MIPR method has a better model fit (lower RMSE) than that of the MIR model, for both shallow and deep water cases. This is due to the split of data into groups of similar behaviour, thereby increasing the consistency of each of the datasets and consequently increasing the reliability of the models representing them.

6.2. Recommendations

Below stated is a list of recommendations, aimed at future development of the research presented in this thesis study.

6.2.1. Tensioner modelling

The *tensioners* are a crucial part of the governing pipelay system and therefore need to be modelled accurately. The motions of the vessel affect the suspended length of the catenary and therefore alter the tension in the pipeline. Appropriate tensioner modelling will result in a good representation of tensioner behaviour offshore, increasing the confidence of the maximum strain outputs predicted by the pipelay model. Therefore, a detailed study of the relation between vessel motions and tension is recommended for better modelling of tensioners.

6.2.2. Validation study

The methods formulated in this thesis study needs to be validated for non-standard vessel motion/sea-state spectra, which is the end goal of this research, but this could not be achieved due to the lack of time. This validation is to reassure the applicability of the models for a *generic* case of vessel motion inputs. Also, the conclusions drawn from the validations in this document only represent a small sample of the infinite combinations of sea-states/vessel motions present in reality. Validation with a larger dataset of motion inputs will help in drawing stable conclusions about the reliability of the models.

6.2.3. Model improvements

The models developed in this thesis study reliably predict the strain outputs. However, there are some improvements that can be done to not only improve the accuracy of predictions, but also provide a theoretical background that helps in the better understanding of vessel motions and their influence on the pipe response. Below listed are a few action points that can be further looked into:

- The database generated for the pipelay model is known to contaain a certain amount of heterogeneity in behaviour, depending on the installation case considered. Splitting of the database helps in grouping of datasets with similar behaviour, thereby increasing the reliability of models that are fit to these separate datasets. This thesis study assumes a split of data along the median of the dominating variable extrema. However, a better understanding of the difference in behaviour of the system over the entire database will help in ensuring an optimal split of the database into two or more groups, enabling the prediction reliability to be improved.
- Currently, every installation case is assumed to have a single dominating variable for the entire database. The split of database is based on this dominating variable. After the split of database, both the new datasets are currently assumed to have the same dominating

variable, based on which, the window is chosen for the MIPR method. However, it is more likely that different datasets will have different dominating variables and therefore choosing the regression window (for recording inputs) based on separate dominating variables will lead to better outputs than when a single dominating variable is used for all datasets. This aspect can be improved for better model reliability and a better understanding of system behaviour.

- The spread function developed in this study is a good way to choose the input-output combination with the best correlation (least spread/dispersion in scatter). This spread function can be further improved to focus on the dispersion of values for specific regions of interest (the regions at which the pipeline integrity is a threat), such that the reliability of the model can be improved in this particular area of interest. This can either be done by concentrating the windows on a particular region of interest, or by assigning higher weight to the window at the required region.

6.2.4. Sensitivity study

The model developed is for a single installation case in a given water depth, with a given pipe, a given set tension along with the assumption of a flat sea bed. In reality however, all the parameters vary as the vessel lays pipe along the route prescribed. It can already be said that the results will be highly sensitive to the bottom tension variation, as changing bottom tension will change the entire static configuration of the catenary, causing it to behave differently. Therefore the effect of these changing parameters on the model output needs to be evaluated, in order to make approximations for such variations.

Also, the number of cases currently simulated in the database are high, since rich data was preferred at the start of this study, in order to develop reliable models. however this richness of data comes with a cost of computation time. Therefore, an optimal dataset generation method is required such that reliable results are produced for a minimal database.

Bibliography

[1] DNV. *Submarine Pipeline systems*. Det Norske Veritas AS, October 2013.

[2] Shunfeng Gong, Pu Xu, Sheng Bao, Wenjun Zhong, Ning He, and Hui Yan. Numerical modelling on dynamic behaviour of deepwater s-lay pipeline. *Ocean Engineering*, 88: 393–408, 2014.

[3] Leo H Holthuijsen. *Waves in oceanic and coastal waters*. Cambridge University Press, 2010.

[4] Gullik Anthon Jensen. *Offshore pipelaying dynamics*. PhD thesis, Norwegian University of Science and Technology, 2010.

[5] JMJ Journée and WW Massie. *Offshore hydromechanics*. TU Delft, 2000.

[6] George Katsikogiannis. Pipeline rotation analysis and modelling during s-lay installation. Master's thesis, Delft University of technology, 2014.

[7] Wouter Liem. Tensioner modelling in pipelay. Master's thesis, Delft University of Technology, 2012.

[8] Orcaflex Manual. Online at http://www. orcina. com/softwareproducts/orcaflex/documentation. *OrcaFlex. pdf*, 2012.

[9] A.V Metrikine. Dynamics, slender structures and an introduction to continuum mechanics. Lecture notes, CT4145.

[10] John Nonemaker. An investigation into the modelling and control of pipeline tension. Master's thesis, Delft University of Technology, 2012.

[11] E Torselletti, R Brusci, L Vitali, and F Marchesani. Lay challenges in deep waters: technologies and criteria. In *Proceedings of the 2nd International Deepwater Pipeline Technology, Clarion Technical Conference, New Orleans, Louisiana*, 1999.

[12] Jeroen van Aubel. *EA-RP-017*. Allseas Engineering B.V., 2015.

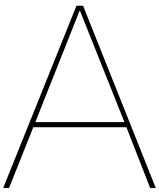

Pipelay terms and definitions

During pipelay operations specific terminology is used to clarify parts and angles of the pipe, stinger and barge.

Tensioners Tensioners are the main element of the pipelay system. Their function is to hold the pipe in suspension between the end of the stinger and the seabed, by applying a constant tension to the pipe.

Firing Line The firing line is the main line from where the pipe joints pass before they leave the vessel. It contains the welding, coating and non-destructive testing stations.

Stinger Stinger is a steel construction attached on the end of the firing line on the front or stern of the vessel. The purpose of the stinger is guiding the pipeline in a pre-determined curve through the water to the seabed.

Stinger radius The stinger radius is the radius of a circle formed by the pipe supports on the stinger.

Lift-off point The lift-off point is the point from where the pipeline is no longer in contact with rollers on the stinger.

Lift-off angle Is the angle of the pipeline, relative to the horizontal plane, at the point where the pipe is no longer in contact with the rollers on the stinger.

Departure angle Is the angle of the pipeline, relative to the horizontal plane, at the stinger tip.

Touchdown point The touchdown point is the point of contact of the pipeline on the sea-floor.

Overbend Overbend is called the pipeline section where the pipe is bent up toward the sea surface. At the overbend region the pipe is guided by the stinger.

Sagbend Sagbend is called the pipeline section where the pipe is bent down toward the seabed (part of the pipeline in suspension). This is between the inflection point and the touchdown point.

Inflection point It is the transition point between the overbend of the pipeline and the suspended pipeline in the sagbend. At the inflection point the moment in the pipeline is zero.

Bottom tension The bottom tension is the axial tension in the section of the pipeline where it touches the seabed. Touchdown point The touchdown point is the point where the pipeline touches the seabed.

Vessel Force The vessel force, applied from the thrusters, is the force necessary to keep the pipeline under tension. This force is equal to the bottom tension